4-2021

Validating Geoclaw for Simulating Teton Dam Failure by Comparison with HEC-RAS Results and Historical Observations

Hannah R. Spero
Boise State University

VALIDATING GEOCLAW FOR SIMULATING TETON DAM FAILURE BY COMPARISON WITH HEC-RAS RESULTS AND HISTORICAL OBSERVATIONS

by

Hannah R. Spero

A dissertation

submitted in partial fulfillment

of the requirements for the undergraduate thesis in

Bachelor of Science in Geoscience - Hydrology

Boise State University

April 2021

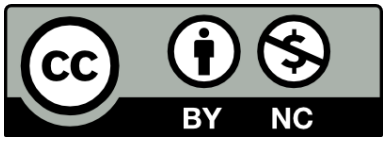

BOISE STATE UNIVERSITY DEPARTMENT OF GEOSCIENCES

UNDERGRADUATE THESIS DEFENSE COMMITTEE AND FINAL READING APPROVALS

of the thesis submitted by

Hannah R. Spero

Thesis Title: Validating GeoClaw for Simulating Teton Dam Failure by Comparison with HEC-RAS Results and Historical Observations

Date of Final Oral Examination: 7 May 2021

The following individuals read and discussed the dissertation submitted by student Hannah R. Spero, and they evaluated the student's presentation and response to questions during the final oral examination. They found that the student passed the final oral examination.

Donna Calhoun Ph.D.	Chair, Supervisory Committee
Michael Schubert HDR Inc.	Member, Supervisory Committee
Jim McNamara Ph.D.	Member, Supervisory Committee

The final reading approval of the thesis was granted by Donna Calhoun Ph.D., Chair of the Supervisory Committee. The thesis was approved by the Department of Geosciences; Chair Professor Jim McNamara.

DEDICATION

This thesis is dedicated to my grandfather, Michael Spero, who was a Army Corps of Engineers and U.S. Bureau of Reclamation Engineer and built dams on the Columbia River. Although he is no longer with us, his curiosity, his love of the outdoors and engineering, and his support are omnipresent.

ACKNOWLEDGMENT

Thank you to my family, my peers, my colleagues, and my mentors for your support and encouragement that allowed me to pursue my interest in geosciences research.

Thank you to my three committee members, the Boise Center Aerospace Laboratory and Josh Enterkine, the Idaho Technical Committee of the Northwest Regional Floodplain Managers Association, the Idaho Section of the American Water Resources Association, Quadrant Consulting Inc., the Boise State Hazards and Climate Resilience Institute, and countless others for their involvement and support of this research. I would like to thank the Bureau of Reclamation and the Department of the Interior for allowing access and reproduction of their drone photogrammetry data and historical records.

I would like to acknowledge the contribution of both NSF (National Science Foundation) Research Grant Award 1819257, "Parallel, adaptive Cartesian grid algorithms for natural hazards modeling" and the Association of State Floodplain Managers scholarship funding through the Annual Student Paper Competition program.

I acknowledge that the Teton River Canyon site area was home to the Shoshone and Bannock Indigenous peoples in the early 1800s. Per the "The Policy of the Shoshone-Bannock Tribes for Management of Snake River Basin Resources" the Shoshone-Bannock Tribes are acknowledged as the previous owners of the ceded

lands of the Teton River Canyon study area.

ABSTRACT

The combination of dams degrading with age and other factors like climate change, technical errors, and human errors lead to dams breaching and failing worldwide. In the United States, over 40,000 dams pose a threat to downstream inhabited areas and constitute a widespread hazard if they were to breach. Therefore, it is critical to accurately predict the resultant floods' downstream flow behavior to create a more resilient community. By improving research, we can concurrently develop and improve mitigation strategies for downstream communities. This study benchmarks the GeoClaw numerical modeling software with the well-documented 1976 Teton Dam failure. A vital tool in dam failure research is two-dimensional (2D) coupled numerical hydrodynamic modeling for dam-breaks. This study aims to benchmark the GeoClaw software, a 2D hydraulic model with novel adaptive mesh refinement (AMR) capabilities (http://www.clawpack.org/) for dam failure analysis by a systematic comparison of dam breach inundation response to both historical data and the industry-standard software HEC-RAS (Hydraulic Engineering Center - River Analysis System).

The objectives of this study are to:

1. Determine the suitability of the GeoClaw software based on its capability to resolve inundation extent and flood front arrival times

2. Compare an instantaneous dam breach with a time-dependent breach formation

3. Quantify the uncertainty of the HEC-RAS model through a sensitivity analysis

This study concludes the 2D GeoClaw dam break model verified by its stability and accuracy, conservation properties, and calibration with the historical hydrological data and HEC-RAS results at a low computational cost. The overall performance of GeoClaw indicates that it is a validated tool for the simulation of dam-break waves in real-cases with future work. The outcomes of this study will assist dam owners, floodplain managers, and emergency managers alike by providing an additional tool for estimating the impacts of dam failures.

TABLE OF CONTENTS

LIST OF FIGURES

LIST OF TABLES

CHAPTER 1:

INTRODUCTION

Dam failures cause some of the most significant disasters associated with the failure of human-made systems in the United States. Through continuous monitoring and mitigation of these dams, communities and dam owners can improve their understanding, building community resilience. Dam failures are an increasingly frequent occurrence worldwide and especially prevalent in the United States; downstream populations are at risk if these dams were to fail. The Association of State Dam Safety lists that there are 84000 dams in the United States that impound about 600000 miles (965606 kilometers) of rivers (ASDSO, 2021). More than 65% of dams are privately owned, and many private dam owners lack the financial resources necessary for adequate dam maintenance (Stanford University, 2018; ASDSO, 2021; Reclamation, 2008). Of those dams, there is an average of ten reported failures every year in the United States. With the current monitoring tools in place, catastrophic dam failures continue to occur, such as the Edenville Dam and Sanford Dam failures in Michigan, United States. Furthermore, the aging dam population is expected to increase failures exponentially over the next thirty years (Stanford University, 2018).

The Teton Dam earthen dam failure provides a unique benchmark problem because of its historical importance, topography, and a wealth of data associated with the

event. On 5 June 1976, the Teton Dam failed and caused the deaths of 11 people, and cost the Federal government close to $400 million in damages (ASDSO, 2021). The Bureau of Reclamation and the United States Geological Survey (USGS) documented the event and personal narratives. The flood from the Teton Dam is initially encapsulated within the Teton Canyon (Magleby, 1981; Reclamation, 2000). However, then the canyon opens onto farmland that is mainly flat. Therefore, this benchmark problem allows for testing a uniform Manning's n (surface roughness coefficient) and handling of two incredibly different domains within the topography. With the suitable data set, historical importance, and interesting topography, the Teton Dam earthen dam failure provides value as a software validation problem and study site.

Consequently, there is a need for advanced and updated software to model the behavior of these dam failures. This study uses GeoClaw, an academic software that models shallow water equations (SWE) with the distinctive ability to refine a 2D mesh adaptively. With the larger domain of the Teton Dam site (55 miles x 27 miles; 88.5 km x 43.5 km), GeoClaw refines flood progression over topography efficiently by focusing on increased resolution only where the water is located. GeoClaw is a potential tool for dam failure modeling demonstrated in the Malpasset Dam failure model and for an outburst flood model (George, 2011; Turzewski *et al.*, 2019). Therefore, GeoClaw represents a cutting-edge tool for dam failure management and, with validation, can be used to understand the downstream consequences of dam failure better.

This research adapts a state-of-the-art software, GeoClaw, for dam failure modeling while exploring tangential unanswered questions that further the field of dam

research (breach importance and uncertainty). This application of GeoClaw provides a new, efficient, and robust method for tracking a dam breach flood downstream with a focus on wave translation and attenuation. The methodology of parameterizing both a time-dependent failure and an instantaneous breach also fills a critical knowledge gap, investigating if the type of breach controls the solution. Furthermore, this study establishes a new benchmark dam failure problem for software validation and provides criteria for comparing software for dam failure analysis in the context of the Teton Dam failure.

Validation and benchmarking of the modeling methods are essential because we can then evaluate how the simulation compares to historical (true) values. Before software can be used for forecasting dam failures for downstream consequences, it must demonstrate usefulness through the capability of estimating peak flow rates and time of peak flow rates, flood wave arrival times, and wave depth with precision and accuracy. Precision in dam numerical modeling means that each time a software computes a simulation with the same input data, it obtains the exact same numerical results (USACE, 2021). Accuracy is defined as similarity to historical values, HEC-RAS values, and demonstration that the foundational equations for each simulation component are solved correctly (USACE, 2021). This study develops the test case of the Teton Dam failure for practical benchmarking and validation of the GeoClaw software – and can be used throughout the modeling community. This study focuses on model validation of the instantaneous dam breach GeoClaw simulation compared with the instantaneous and time-dependent HEC-RAS simulations.

The motivations for this research are twofold, both societal and scientific in

importance. Studying the extensive and costly consequences of major rapid flooding events, like dam failures, requires accurately predicting flow velocities, water depths, and flood arrival time. Hence, the scientific motivations behind this research are to improve modeling and forecasting tools by benchmarking a low-cost and flexible approach through the GeoClaw software; this allows for an improved understanding of model parameterization and how it affects downstream consequences.

This research is also motivated by the societal need to understand downstream flow dynamics better, define better mitigation strategies, and improve a community's understanding of this human-made hazard. When facing catastrophic situations, downstream communities can use this numerical modeling software for flooding. Understanding dam failure downstream flooding will have profound societal impacts and implications -including improving mitigation, updating evacuation plans, expanding inundation mapping, identifying downstream consequences, and performing better risk evaluations. Ten years ago, only about 1000 dams posed a risk to downstream populations, but in the last decade, now 14000 pose a risk (FEMA, 2013). Through this dam failure model, millions of at-risk downstream lives can have access to safety measurements, such as knowledge and modeling, that will save lives.

1.0.1 Guiding Questions

Assessing the suitability of GeoClaw for dam failure modeling is critical as a potential tool for evaluating the downstream consequences of a flood that results from a dam breach. To gauge this, there are three guiding questions in this study that focus on evaluating the GeoClaw model for dam breach model capabilities. The suitability of GeoClaw for dam failure modeling is first assessed through evaluating

the Teton Dam failure model. The criterion for success includes similarity of GeoClaw model flood arrival times, inundation extent, and flow depths to historical data. This study also compares the underlying mathematical solution of GeoClaw to HEC-RAS as the mathematics control the flood movement. Then, the ease of use, pre-processing and post-processing, and other performance characteristics are evaluated. GeoClaw utilizes an instantaneous dam breach assumption, so this study uses a sensitivity analysis with the HEC-RAS model to calculate the importance of the assumption of an instantaneous breach against a time-dependent breach. Evaluating the importance of the dam breach also furthers existing scientific understanding. We decide the breach progression assumption is invalid if there are notable differences between model values for peak flow rates and flood wave peak flow times. Furthermore, this study investigates what parameters control the solution by determining the uncertainty of the constructed HEC-RAS model, improving the current threshold of industry knowledge.

1. Is the GeoClaw model suitable for dam failure downstream modeling?
    (a) Mathematical formulation controlling flood movement
    (b) Capability to predict inundation extent and final flow depth through a numerical method
    (c) Ease of use, performance characteristics, and tools for visualization and post-processing
2. What is the importance of breach progression in numerical modeling?
3. What is the uncertainty associated with using HEC-RAS for this benchmark problem?

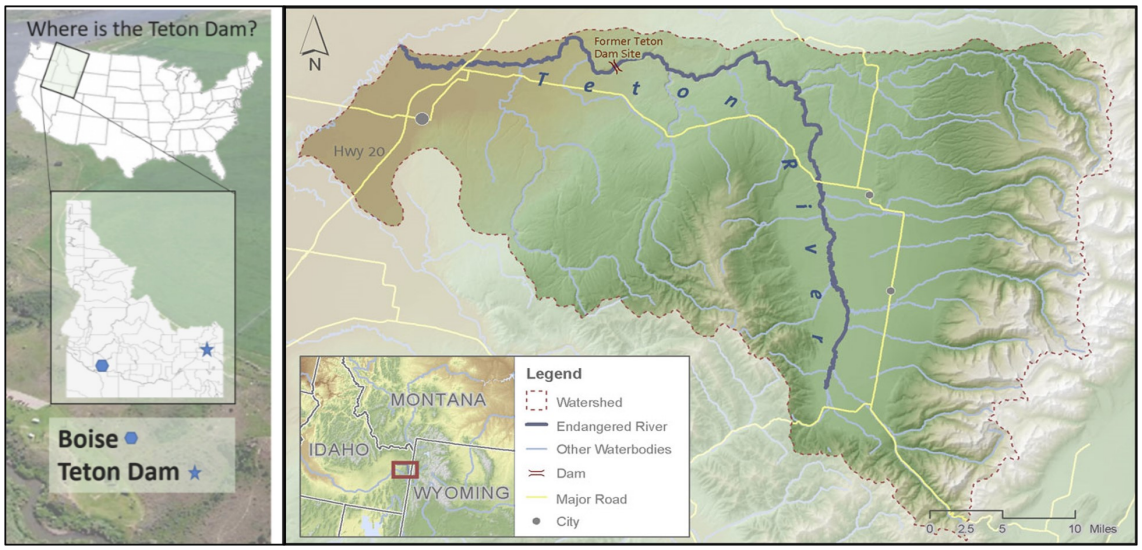

Figure 1.1: (Left). Location of Teton Dam on United States and within state of Idaho. (Right) Amended figure of the Teton watershed containing Teton River with the red text denoting the location of the historic Teton Dam.

1.1 Background

1.1.1 Geologic Setting and Site Information

The Teton Dam Site consists of the Teton River Canyon and the Teton Dam, both in Eastern Idaho, United States 1.1. The geologic study area of the Teton River canyon is bounded between Rocky Mountain overthrust and the younger Snake River Plain downwarp; the volcanic plateau denoted the Rexburg Bench (Reclamation, 2000). This area contains volcanic deposits, evidence of the Yellowstone hotspot track (Pierce *et al.*, 1992). Tributaries to the Teton River in the study area include Bitch Creek and Badger Creek, which drain from Grand Teton National Park (20 miles (32 km) to the East) (USGS, 1976). The Teton River has extensively eroded the intracanyon Huckleberry Ridge tuff and underlying

basalt flows (Magleby, 1981). In general, the Teton River canyon is narrow at the upstream end (RM 19), and the canyon becomes gradually wider downstream with a decreasing slope (Magleby, 1981; Reclamation, 2000). Due to the river's steep canyon walls and consistent erosion, landslides are considered a natural process on the Teton Canyon (Reclamation, 2000).

The Teton Dam is on the Teton River, which passes through the Fremont and Madison counties of Idaho. The Bureau of Reclamation commissioned the dam to provide irrigation and flood control along with wildlife mitigation measures. They designed the 17-mile-long (27 km) reservoir to have a total capacity of 288000 acre-feet ($3.5e^8$ m^3) volume and a surface area of 2100 acres (8.5 km^2) (Reclamation, 1976). The Teton Dam was commissioned originally to provide supplemental irrigation water for approximately 110000 acres (445 km^2) in the Fremont-Madison Irrigation District for flood control operations Schuster & Embree (1980); Reclamation (2000).

1.1.2 Teton Dam Failure

Public Law 88-583, on 7 September 1964, authorized the building of the Teton Dam (Reclamation, 1976). The Bureau of Reclamation began building in 1972, and by 1975 the dam was filling. However, in early 1976, the reservoir was filling rapidly due to early and high inflows from a heavy snowpack upstream. The reservoir inflow was 4000 cfs (113 m/s) in mid-May. The Teton Dam's main river outlet works in the left abutment (pool capacity 3400 cfs; 96 m/s) were not operational as the manufacturer had not received a regulating gate. Therefore, the only outlet was in the right abutment, the auxiliary works, with a capacity of 850 cfs (24 m/s) (Land, 1980; Reclamation, 2006). On 3 June 1976, when the reservoir was at 5300 ft. (1615

Figure 1.2: The historic Teton Dam Failure documented by the Bureau of Reclamation photos occurring at (A) 11:30, (B) 11:40, (C) 11:57, (D) 12:05 occuring on 5 June 1976 (Reclamation, 1976).

m) elevation (NGVD 29; Appendix Table 1: Datum Conversions), two seeps flowing 60 (0.1 m/s) and 40 gpm (0.09 m/s) were found at 1,300 (396 m) and 1,500 feet (457 m), respectively, downstream of the dam at the base of the right abutment. Then, at 7:00 5 June 1976, a survey party observed a leak coming from the right abutment at the top of the berm at elevation 5045 ft (1538 m; NGVD 29). Between 10:00 and 10:30, a wet spot had formed at elevation 5200 ft (1585 m) (1.2; NGVD 29), 20 feet (6 m) above the base of the right abutment. At 10:30, a roar was heard as the water began to burst through the dam. At 11:00, a whirlpool had formed in Teton Reservoir 150 feet (45.7 m) from the right abutment, rapidly expanding. Next, at 11:50, a sinkhole developed on the downstream slope shortly before the embankment crest collapsed at 11:55; the dam breached two minutes later at 11:57. By between 17:00 - 18:00 the reservoir had emptied (Reclamation, 1976).

The Teton Dam failure was a catastrophic event caused by a piping failure. It destroyed downstream communities and took lives. At the time of failure, the reservoir was at an elevation of 5301.7 ft (1616 m; NGVD 29) about 272 ft. (82.9 m) deep at the dam and filled approximately 250000 acre-ft ($3.1e^8$ m^3) of water, but later estimates calculated the volume at 234000 acre-ft ($2.89e^8$ m^3) using NAVD 88 (Reclamation, 2000, 2006, 2008). Total reservoir capacity would have had a water

surface elevation of 5327.9 ft (1623.9 m) (NAVD 88) forming, 288250 acre-ft ($3.56e^8$ m^3) of stored water (Reclamation, 2006). The Teton Dam failure was determined to have occurred due to a piping failure causing the embankment material to fail(Reclamation, 2000). The destruction downstream from the dam was extensive, reaching the upper end of American Falls Reservoir, 95 miles (153 km) downstream (Reclamation, 2000).

Other implications from the Teton Dam failure include a significant change in the geomorphology of the canyon. According to Reclamation's Geomorphology report 2000, the Teton Dam failure activated more than 200 landslides (Schuster & Embree, 1980; Reclamation, 2000; Carter, 1976). In total, these landslides submerged the reservoir, 500 acres (2.02 km^2) of material failed, and approximately 3.6 million ft^3 ($1.02e^9$ m^3) of debris moved to the canyon floor (Magleby, 1981). These landslides pose a challenge in numerical modeling of the Teton Dam, as all digital elevation models (DEMs) host the new reservoir characteristics, decreasing the volume of water that can be stored in the model's reservoir.

1.1.3 Parameterizing a Benchmark Problem

The Teton Dam was chosen as the benchmark problem for validating GeoClaw for dam failure modeling because the dam and the failure were well-documented by the Bureau of Reclamation, the USGS, and local civilians, allowing for a database describing the event. Therefore, the Teton Dam failure provides sufficient documentation to prepare a benchmark problem for evaluating the GeoClaw numerical algorithms' effectiveness for dam-break modeling. In this context, GeoClaw is tested by modeling the historic Teton Dam dam-break flood. This earthen dam explosively failed by piping, suddenly on 5 June 1976, emitting a peak

dam failure outflow of 2300000 cfs (65128.7 m/s) (USGS, 2021).

The Teton Dam was one of the tallest dams in the United States in 1976, with a crest 300 feet (91 m) in height. The length of the crest was 3000 feet (914 m), and the width of the crest was 35 feet (11 m). This dam stored a volume of 288000 acre-ft ($35.5e^8$ m^3; NGVD 29) along the Teton River, only reaching 234,260 acre-ft (28.9 e^8 m^3)before failing (Reclamation, 2006). However, as the dam was filling at 4 ft (1.2 m) per day (Reclamation, 1976), a thousand times faster than the engineers had planned initially, the groundwater inflow affected the dam's impervious core, which cracked from hydraulic fracturing. This inflow generated three springs that were found downstream on 3 June 1976. The earthen Teton Dam failed on 5 June 1976, in Eastern Idaho at 11:57. Teton Dam failure's downstream consequences (**??**) included 70 miles (113 km) of flow downstream, eleven deaths, and over 2.9 billion dollars of damage (Reclamation, 1976).

Table 1.1: Historical data for downstream locations with corresponding flood depth, arrival times (on 5 June, 1976), and distance from the dam; sourced from historical records Reclamation (1976); USGS (1976).

Location	Distance [1]	Arrival Time [2]	Peak Flow	Max. Depth [3]
Teton Canyon	2.51 mi / 4 km	12:05	2300000 cfs / 65128.7 m/s	49 ft / 15 m
Teton Canyon Mouth	4.97 mi / 8 km	12:10-12:20	X	39 ft / 12 m
Wilford	8.42 mi / 13.5 km	12:45	X	13 ft / 4 m
Teton Town	8.00 mi / 12.9 km	12:30	1060000 cfs / 30015.8 m/s	9.8 ft / 3 m
Sugar City	12.3 mi / 19.8 km	13:30	X	9.8 ft / 3 m
Rexburg	15.2 / 24.6 km	14:30	X	8,2 ft / 2.5 m

(1) where 'distance' refers to the distance from the dam to the historical observation location (2) where 'arrival time' refers to the flood wave arrival time on 5 June 1976 in 24-HR clock time (3) where 'max. depth' refers to the maximum flood wave depth in the historical observation location

1.2 2D Numerical Modeling Software

1.2.1 GeoClaw Software

This study used GeoClaw (v.5.8), part of the open-source software package Clawpack based on the Clawpack Conservation Laws Package benchmarked for solving geophysical flow problems (Clawpack Development Team, 2020; Mandli *et al.*, 2016). GeoClaw has been used in previous studies for storm surge, outburst floods, debris flow, and extensive tsunami modeling research (Mandli & Dawson, 2014; Mandli *et al.*, 2016; George, 2011; Turzewski *et al.*, 2019; MacInnes *et al.*, 2013; Arcos & LeVeque, 2015). The GeoClaw software was developed in 1994 and has been extensively tested and validated (González *et al.*, 2011). GeoClaw was initially developed for tsunami modeling derived equations from integrating 3-dimensional (3D) governing equations in the vertical direction, thus reducing the simulation to a time-dependent, two-dimensional computation (2D) depth-averaged shallow water equations (SWE; $http://www.clawpack.org/geoclaw.html$). The SWEs are widely accepted as the mathematical formulation for resolving dam failure flood regimes. They best combine computational efficiency and accurate reconstruction of real-world flow regimes. General agreement exists that SWE can be used to describe dam-break waves over natural topography (Hervouet & Petitjean, 1999).

Adaptive Mesh Refinement (AMR) is a chief advantage of GeoClaw compared to other software as it allows for the efficient solution of multi-scale flow problems (Berger *et al.*, 2011). AMR is a feature built into GeoClaw, which controls the solution's refinement by computing where the solution is sensitive. This method is

dynamic, meaning that as the simulation progresses and turbulent or sensitive areas of the solution change, the level of grid refinement in these areas also changes – patch-based refinement on logically rectangular Cartesian grids. AMR in GeoClaw uses refined grids in areas where the water height is non-zero and coarser grids on dry land or over areas where flooding has not yet occurred 2.5. AMR allows for efficiency and accuracy in modeling solutions that vary temporally and spatially, such as dam failure downstream modeling.

The GeoClaw software models wave propagation by solving systems of hyperbolic partial differential equations. For dam breach downstream modeling, GeoClaw solves the depth-averaged 2D SWE equations derived by integrating the 3D governing equations in the vertical z-direction from the solid bed b(x, y) to the free surface n(x,y,t) of the flow and applying boundary conditions at those surfaces. This solving mechanism gives the new governing equations of the model for depth (h) and the depth-averaged velocities in the x- and y- directions, respectively (George, 2008, 2011).

As the flood wave propagates forward in time through cell-to-cell transfer, the numerical solution is updated based on time steps at that cell interface (Calhoun & Burstedde, 2017). A rectangular computational domain, such as the Teton Dam domain, inevitably contains both wet and dry cells in flood-routing problems. Therefore, another critical component of the GeoClaw numerical method that resolves a moving wet-dry front of the flood, which is resolved using the Reimann solver. As these fluxes at the cell interfaces cause hyperbolic problems that must be solved for local Reimann solver, GeoClaw employs the Godunov-type scheme for solutions to local Riemann problems (Godunov & Bohachevsky, 1959). Using the

classical Godunov approach for solving hyperbolic conservation laws, GeoClaw can resolve hydraulic jumps and shocks within the domain by solving conservation laws at each cell interface, allowing for a superior result that can be computed efficiently. More details of these numerical methods can be found in George 2006; 2008 and LeVeque et al. 2011.

Since it is impossible to determine exact analytical solutions to the SWE in the presence of general two-dimensional topography, validation of numerical methods for terrestrial floods over terrain can only be computed by comparing empirical data from physical floods other previously validated codes.

1.2.2 HEC-RAS Software

The first version of Hydrologic Engineering Center's River Analysis System (HEC-RAS) Version 1.0 was developed in 1995 (Brunner, 2016). In the most recently released version (5.0.7), HEC-RAS has the novel capabilities of performing fully 2D computations based on 2D fully dynamic equations and the 2D diffusion wave equations (USACE, 2019). It also offers the opportunity to perform 1D/2D coupled simulations or 2D/2D coupled simulations to take advantage of a simulation-benchmarked (USACE, 2019; Brunner *et al.*, 2015). HEC-RAS has been used for dam breach modeling and is considered an industry standard. For example, Patel *et al.* (2017) reproduced the flood event induced by the water volume released from the Ukai Dam (India); highlighted the broad capabilities of HEC-RAS 5.0.7 for flood modeling and inundation mapping studies from dam failure. HEC-RAS has been used as a benchmark model to test the performances of other models. HEC-RAS is accessed through a graphical user interface (GUI) and solves the fully 2D shallow water equations (SWE) (Costabile *et al.*, 2020).

Within the gridding of HEC-RAS 5.0.7, the Courant-Friedrichs-Lewy (CFL) condition is implemented as well for user-determined time-step to ensure the model's stability (Brunner, 2002). The CFL is the stability criteria value where numeric solutions to partial differential equations are used (PDEs). The CFL is a dimensionless number representing proportional relationships between time-step, velocity, and grid cell size.

1.2.3 Comparison of HEC-RAS to GeoClaw

It is important to note specific differences between the HEC-RAS software and the GeoClaw software, which will be accounted for in this research. Some key differences between the two software are the numerical schemes, interactive GUI, and mesh parameterization, which is either user-defined or auto-generated and adaptively refined (Appendix A.11, A.10, A.12, A.13, A.15, A.14).

1.3 Previous Work

1.3.1 1977 Gundlach and Thomas

In 1977 the Bureau of Reclamation used a preliminary version of HEC-RAS (USTFLO; a Gradually Varied Unsteady Flow Profiles model) to investigate the Teton Dam failure (Land, 1980). They used a 1D model with horizontal water surface traverse to the flow to model the failure because a 2D model was not feasible in 1976 as they lacked computational resources (Gundlach & Thomas, 1977). The model was parameterized with an instantaneous flood development sequence and full dynamic routing to perform breach analyses (Land, 1980). Without the computational resources necessary for 2D modeling, they produced a 1D model output.

Table 1.2: Comparison of HEC-RAS and GeoClaw softwares.

Comparison Characteristic	GeoClaw	HEC-RAS
Developer	University of Washington	U.S. Army Corps Engineers
Adaptive Mesh Refinement	Yes	No
Mathematical Scheme	Explicit FV	Implicit FV
Shock-Capturing	Yes	Yes
1D/2D Linkages	Yes	Yes
Parallel Capabilities	Yes	Yes
Mesh Shape	Quadrilateral Block-Structured	Polygonal Cells, User-Defined
Interactive GUI Interface?	No	Yes
Variable Manning's Roughness	No	Yes

Location	Miles Downstream from dam (A)	Date (month, day, and year)	Arrival time (hrs)	Elapsed time between sites (minutes)	Approximate mean velocity between sites (ft/min)	Approximate mean velocity between sites (mi/hr)
Teton Dam	0.0	06/05/1976	11:57 AM	---	---	---
Teton Canyon	3.0	06/05/1976	12:05 PM	8	1980	23
Teton Town	8.8	06/05/1976	12:30 PM	25	1220	14
Sugar City	12.3	06/05/1976	1:00 PM	30	620	7
Rexburg (B)	15.3	06/05/1976	1:40 PM	40	400	5
Henry's Fork (near USGS gauging station)	22.6	06/05/1976	3:30 PM	110	350	4

Figure 1.3: Estimated Times for Leading Edge of Teton Dam Flood Wave based on field observations, (Reclamation, 1976)

.

The 1977 Reclamation model took seven weeks to set up the data and debug the model to perform the dam breach analysis (Gundlach & Thomas, 1977). 5% of the set-up time was used to establish the model's initial base flow conditions and stabilize the computations when a negative surf reached the upstream boundary 1977. Their HEC-RAS study model used the Saint-Venant equations (or shallow water equations) for free surface hydrologic modeling, which most dam failure software uses today(Hervouet & Petitjean, 1999). They also initialized their reservoir with the best estimates of the known volume of water at the time of the failure (Gundlach & Thomas, 1977).

Furthermore, this event has been studied using one-dimensional models and has helped form the basis for the understanding of earthen dam failures Blanton (1977); Snyder (1977); Brown (1977); Fread (1977); Thomas (1977); Macchione & Sirangelo (1990); Gundlach & Thomas (1977); Balloffet & Scheffler (1982).

1.3.2 Teton Dam Idaho National Laboratories 2015 Study

Idaho National Laboratories (INL), Boise State University, and Neutrino Dynamics Incorporated in 2015 modeled a hypothetical and exaggerated Teton Dam failure. This study modeled inundation affecting a fictitious nuclear power plant (Smith *et al.*, 2015). The scenario models a simplistic dam break of the Teton Dam and the resulting inundation of a fictitious Nuclear Power Plant modeled with Smoothed Particle Hydrodynamics (SPH) - a robust Lagrangian approach for simulating fluid flows. The breach was exaggerated to show a dramatic coupling of the flood 2015. This coupling effort was modeled in three stages: (1) 2D GeoClaw simulation, (2) 3D domain of Neutrino Flow, and (3) Inflow to the 3D domain. The GeoClaw set-up used an instantaneous dam failure with a vertical wall of water where the dam was located at an initial water height of 115 m from ground level (377.3 ft) 2015. The GeoClaw results were used as inputs for the one-way coupling to the 2D DualSPHysics SPH open-source code coupled with the 3D SPH area. Neutrino Dynamics Inc. simulated the water flow like a riverine flood in the fictitious nuclear power plant of interest (Smith *et al.*, 2015). However, this work left gaps in knowledge for the application of GeoClaw software for validity.

1.3.3 Malpasset Dam Failure Studies

GeoClaw 2011 Study

The GeoClaw study of Malpasset Dam failure was the first to apply GeoClaw to dam failure modeling, and the methods employed Reimann solvers that were well-balanced concerning steady-state balances to capture the non-stationary flow in the rugged terrain accurately for shallow-water applications (George, 2011). The

preliminary results for the first validation of this code for dam-break flooding problems demonstrated that GeoClaw (Adaptive Cartesian gridding) is a viable alternative to using specially developed unstructured meshes exhibiting minimal computational cost with result accuracy because of AMR's efficiency (George, 2011). This study compared GeoClaw results to Valiani et al. and Hervouet and Petitjean, who used the commercial software package TELEMAC-2D (Valiani *et al.*, 2002; Hervouet & Petitjean, 1999). The comparison concluded that all three numerical simulations had nearly identical results that differed more from laboratory data than from one another (George, 2011).

HEC-RAS 2011 Study

HEC-RAS v.4.1.0 was used to model the Malpasset dam breach benchmark problem compared to 2D modeling software ISIS (Almassri, 2011). In simulating the dam break test, HEC-RAS produced results similar to the historical numerical values. HEC-RAS was concluded to be efficient, fast, and accurate for simulating dam breach. However, both ISIS and HEC-RAS were concluded to require a sizable amount of data input to initiate the models and produce reliable results (Almassri, 2011).

CHAPTER 2:

METHODS

2.1 Approach

This study composes a GeoClaw model for the Teton Dam benchmark problem. We ran the GeoClaw and HEC-RAS software on the same dataset (topography and initial conditions) and determined the GeoClaw model's capability to predict inundation extent by identifying the simulated flood boundary compared with the historical flood outline. This study tracked flood wave arrival times and final flow depth using GeoClaw Lagrangian and stationary gauges inserted into the simulation at points with known historical values.

We consider GeoClaw validated if the lateral extent agrees with the historical perimeter and if gauges demonstrate flood wave arrival times within ± 15 minutes and maximum depths within ± 25 feet (± 7.62 m) of historical depths. The importance of breach progression was determined by means of a HEC-RAS sensitivity analysis comparing an instantaneous dam failure to a time-dependent dam failure using peak flow rate, flood wave arrival time, and time of peak flow. We decide the breach progression is important if there are notable differences between model values for peak flow rates (50000 cfs; 1415.8 m/s) and flood wave peak flow times (± 15 minutes). Three other sensitivity analyses were conducted which used

variations of the base model (instantaneous dam breach) in HEC-RAS, to determine what was controlling the numerical solution and the accuracy of the modeling results.

2.2 Metadata, Model Domain, and Remote Sensing

For this benchmark problem parameterization, horizontal and vertical datum conversions were used to align topographic features to historical values. Two topographies were implemented in this modeling effort, originally sourced from the USGS in projection WGS 84 (2.1; USGS, 2015). The first topography, TetonLarge (6.99 KB), covers the larger study area (2.1), at 98 feet (30 meter) resolution. The second topography, TetonDamLatLong (7.77 KB), covers a smaller area at 33 feet

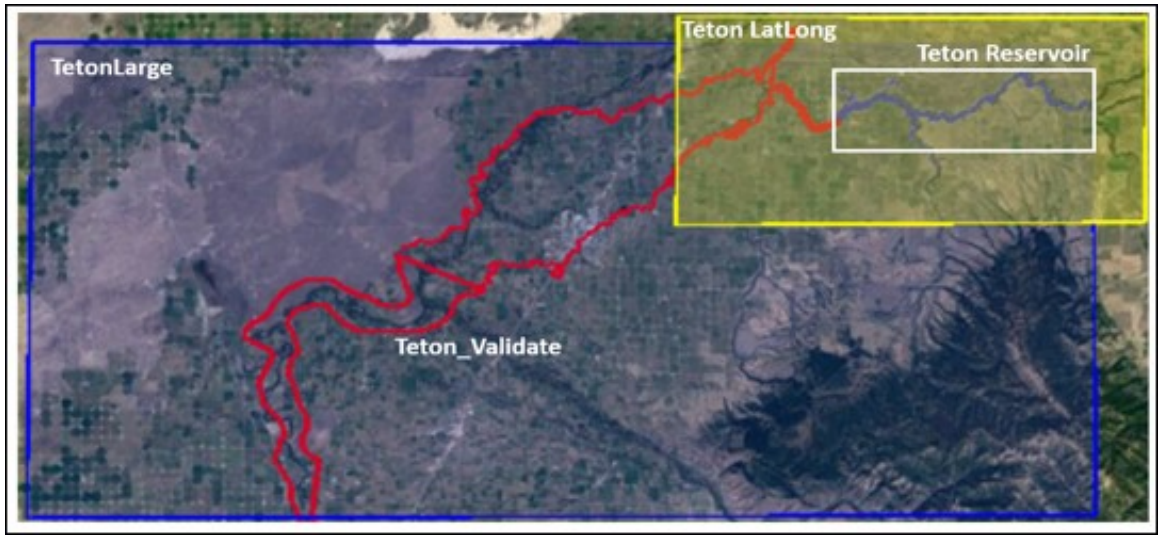

Figure 2.1: TetonLarge and Teton LatLong DEM's along with the detailed Teton Reservoir and the red outline of the historic flood (TetonValidate). The domain extent above is 55 miles base by 27 miles length (88.5 km x 43.5 km).

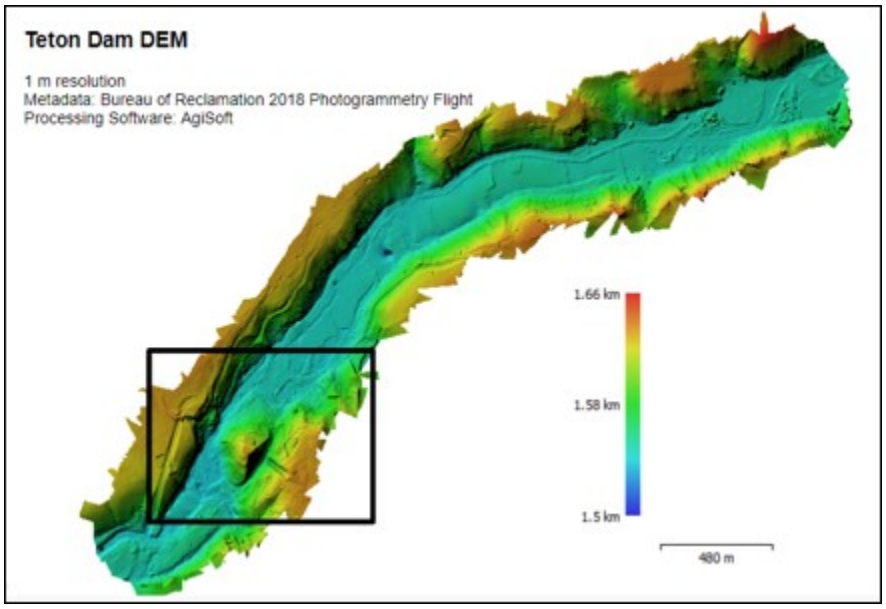

Figure 2.2: TetonDamPhoto.topo processed DEM at 3.28 ft (1 m) resolution with the black box denoting the locating to the Teton Dam failure site.

(10 meter) resolution. Together, TetonDamLatLong and TetonLarge form a 55 x 27 square-mile domain (88.5 km x 43.5 km). For similarity of models, the same topography was used in GeoClaw and HEC-RAS models as metadata (A.2). For the 2D modeling of the flood propagation, this study provides two downloadable files (TetonLatLong.topo and TetonLarge.topo) in an open-source repository associated with this manuscript for open-source access, allowing for reproducible research (Spero, Hannah and Calhoun, Donna and Schubert, Michael, 2021).

This study also generated a high-resolution topography (HRT) from remote sensing methods, using Bureau of Reclamation drone photogrammetry data (Reclamation, 2015). HRTs allow for improved modeling but can add to the model computational cost. The HRT consists of a 1.5 mi^2 area (3.88 m^2) at 3.28 ft (1 m) resolution (TetonPhoto.topo; 2.2). Using Agisoft Metashape software, a dense point cloud was

constructed after aligning photos with 5-million-point density from provided georeferenced photographs LLC (2006). Through optimizing camera alignment and manually cutting out unnecessary or unconnected points, the dense cloud was reduced to 3-million-point density. Photos depicting the river did not align well because of sunlight refraction on the day the drone data was collected, and so the water was cut out of the dense cloud and filled by interpolating points. Following generating the dense cloud, a mesh was built with a height field as surface type, and a DEM was output with a State Plane East FIPS 1101 ft coordinate system specified. An orthomosaic of the Teton Dam site was also exported for a tangential study – communication the Teton Dam failure using Virtual Reality (Spero *et al.*, 2021).

This study was able to use TetonPhoto.topo in HEC-RAS in .TIFF format and exported a terrain with a all three topographies combined (TetonPhoto.topo, TetonLatLong,topo, and TetonLarge.topo). Although TetonPhoto.topo is high-resolution and allowed for initial testing in HEC-RAS, this study's scope did not include an analysis of HRT usage in GeoClaw and HEC-RAS for dam breach modeling.

2.3 Numerical Model Methods

2.3.1 GeoClaw Simulations of Downstream Flood from Dam Failure

The workflow to develop the GeoClaw Teton Dam model consisted of five primary steps: (1) parameterizing the historic reservoir, (2) adapting the code, (3) parameterizing an instantaneous dam breach, (4) maximizing computational

efficiency, and (5) performing a sensitivity analysis for model uncertainties (2.3).

Parameterizing Teton Reservoir

The Teton Dam failure problem defined a region upstream from the dam confined within the reservoir area (file: qinit.f90). A polygon was defined at Teton Canyon's edges, extending 17 RM upstream from the dam site. The 'reservoir path' polygon outlined the historic reservoir as denoted in (Reclamation, 1976) was used to estimate the volume and flow by the Bureau of Reclamation (Reclamation, 1976). These points were plotted at the historic dam height throughout the reservoir – 5327.9 ft (1623.9 m) (NAVD 88; 2.4).

Then, the Teton River for 17 RM was filled with water to 5305.3 ft (1617.1 m) water surface elevation (WSE; NAVD 88). Next, using a reservoir volume estimate through Google Earth and ArcGIS, the validity of the polygon volume for the Teton Reservoir was assessed (Spero, Hannah and Calhoun, Donna, 2020). Using historical parameters for the reservoir, we mapped and calculated the average height and confirmed the model's initial volume to be reasonable. To calculate the volume, an average height was calculated using only level-4 refinement and adding up the volume of each water column on level-4. Measurements differ from (Spero, Hannah

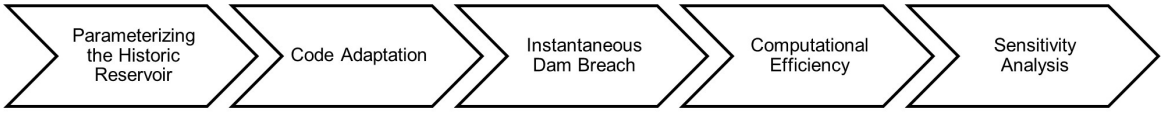

Figure 2.3: The workflow to develop the GeoClaw Teton Dam model consisted of five primary steps: (1) parameterizing the historic reservoir, (2) adapting the code, (3) parameterizing an instantaneous dam breach, (4) maximizing computational efficiency, and (5) performing a sensitivity analysis for model uncertainties.

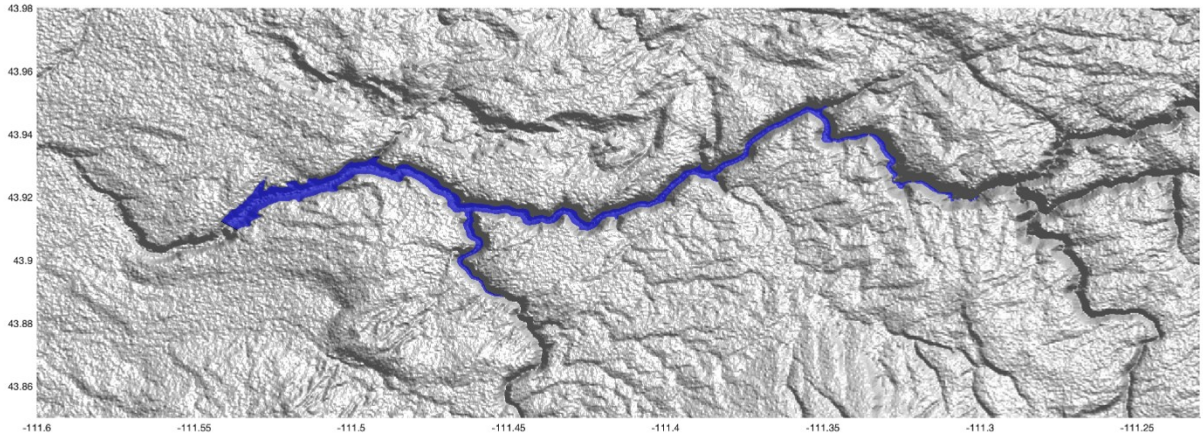

Figure 2.4: Initial GeoClaw simulation set-up for the parameterized reservoir on TetonDamLatLong.topo. The blue denotes the maximum water surface elevation of the reservoir.

and Calhoun, Donna, 2020), with volume results due to increased refinement and no assigned reservoir slope.

The final model demonstrates a volume of 247273 acre-ft (3.05 e^8 m^2), close to the historical value of 234260 acre-feet (2.89 e^8 m^2) (Reclamation, 2006). We consider this suitable, as the historical method to derive volume (end-area method) and the contour topography map (Magleby, D.N., 1981) are not as accurate as our methodology.

Instantaneous Dam Breach Set-Up

Although the breach evolution was reasonably well defined (Reclamation, 1976; USGS, 1976), GeoClaw was parameterized using an instantaneous dam breach assumption, meaning that the first moment with respect to the water surface computed is the time-step following tn. Therefore, the dam instantaneously fails completely following t0 at t1, the first time-step of the simulation; the first step of

the simulation represents the instantaneous removal of the dam.

Adaptive Mesh Refinement

GeoClaw allows the user to specify various parameters controlling AMR refinement criteria before a simulation. For instance, one can enforce refinement by associating minimum flow criteria with a given level, such as the magnitude of the gradient of a solution variable. To accomplish the above refinement scenarios for the Teton Dam failure and resulting flood, the domain was refined to level-4. This ensured that the reservoir was refined enough to provide a reasonable resolution for the mass flux leaving the reservoir and captured the moving flood front at a high refinement level (2.5). The level-4 refinement for the mass calculations (initial GeoClaw volume). For floods where it is desired to capture specific flow features at a higher resolution, such as large gradients near the flow front, more levels, and flow criteria could be used, although this was not within the scope of this research.

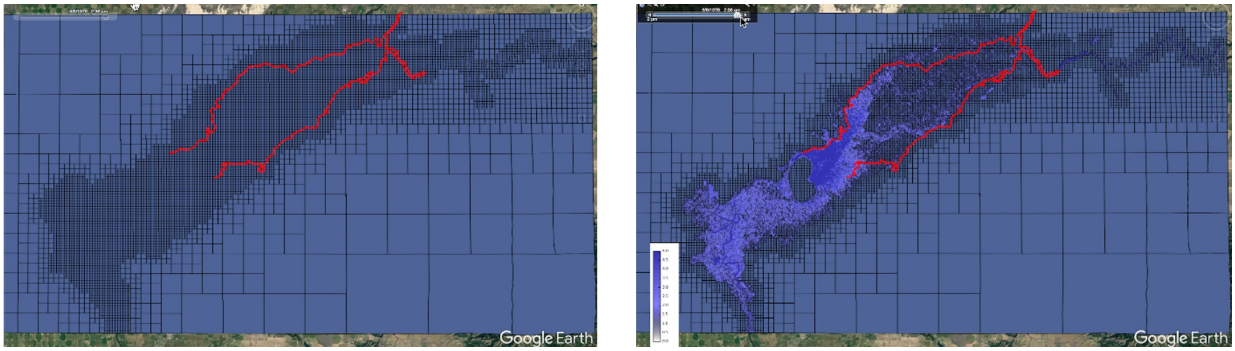

Figure 2.5: Mesh adaption in ForestClaw, a implementation of GeoClaw using quadtree meshes; applied to the Teton Dam domain (Calhoun & Burstedde, 2017).

Parameterizing the Roughness Coefficient

Selection of Spatially and Temporally Uniform Manning's Roughness Parameter, n was a key portion of the model parameterization. The only parameter in the shallow water model that governs friction is the Manning's coefficient and is user-implemented. The Manning's coefficient for the entirety of the study area was determined to be 0.06 from a field expedition. Then, for confirmation of the Manning's n value, we used: Manning's n definitions, gauge data, high watermark data, field interviews, newspaper records, hydrologic comparisons, and verification data (the observed event at the seven gauges) to determine the confidence of 0.06 value (Gundlach & Thomas, 1977). This falls within the recommended literature value range (Chow, 1959).

Stationary and Lagrangian Gauges

Stationary gauges were inserted into the setrun.py and visualized through VisClaw and setploy.py to track the time-series water surface elevation (WSE) at locations with historical data. Stationary gauges output the shallow-water equation solution at a specified location (x,y), which serves as a proxy for comparison with historical records and accounts and log flood wave arrival time and peak flow values. Gauges were denoted as regions of refinement and identified using latitude and longitude (2.6). Gauges were used to compare computational results to measurements from historical accounts as a function of time at a fixed geographical position. We create a series of output images (.png files) that we overlay onto Google Earth for visualization. The color scale on the images is used to depict inundation depth. Another significant way that the fluid continuum was tracked in GeoClaw was

Gauge Name	Stationary Gauge Number	GeoClaw		HEC-RAS	
				ID E 1101	ID E 1101
		Latitude	Longitude	Northing (US ft)	Easting (US ft)
Teton Dam Canyon	Stationary #1	-111.594	43.9341	826,877.67	807,045.17
Teton Canyon Mouth	Stationary #2	-111.666	43.9338	826,644.23	787,947.83
Wilford	Stationary #3	-111.672	43.9144	819,563.55	786,488.67
Sugar City	Stationary #4	-111.76	43.8633	800,810.36	763,391.63
Rexburg	Stationary #5	-111.792	43.8231	786,116.88	754,965.75
Blackfoot	Stationary #6	-112.341	43.1876	554,323.97	609,753.23

Figure 2.6: Stationary Gauges Table with locations for both GeoClaw (latitude and longitude) and transposed Northing and Easting locations for HEC-RAS.

through modeling 3x3 grids of Lagrangian particles/gauges (2.7). Note that this is the first study where Lagrangian gauges were used in GeoClaw for terrestrial flow modeling. The Lagrangian gauges were inserted into setrunparticles.py and visualized through VisClaw using setplotparticles.py (Spero, Hannah and Calhoun, Donna and Schubert, Michael, 2021). The trajectories of the Lagrangian particles demonstrate the fixed velocity at points in space, a Eulerian representation of the flow. The particles are displayed on top of water particles through:

1. The Fundamental Principle of Kinematics (the velocity at a given position and time is equal to the velocity of the parcel that occupies that position at that time)

2. The material or substantial derivative relates the time rate of change observed following a moving parcel to the time rate of change observed at a fixed position, where the advective rate of change is in field coordinates.

Gauge Name	Lagrangian Cluster #1	Initial Latitude	Initial Longitude	Gauge Name	Lagrangian Cluster #2	Initial Latitude	Initial Longitude
Teton Dam Canyon Cluster	Gauge 100	-111.6210	43.9134	Menan Butte Cluster	Gauge 200	-111.9420	43.8006
	Gauge 101	-111.6090	43.9134		Gauge 201	-111.9300	43.8006
	Gauge 102	-111.5970	43.9134		Gauge 202	-111.9180	43.8006
	Gauge 110	-111.6210	43.9233		Gauge 210	-111.9420	43.8106
	Gauge 111	-111.6090	43.9233		Gauge 211	-111.9300	43.8106
	Gauge 112	-111.5970	43.9233		Gauge 212	-111.9180	43.8106
	Gauge 120	-111.6210	43.9333		Gauge 220	-111.9420	43.8206
	Gauge 121	-111.6090	43.9333		Gauge 221	-111.9300	43.8206
	Gauge 122	-111.5970	43.9333		Gauge 222	-111.9180	43.8206

Figure 2.7: Lagrangian Gauges Groups #1 and #2 with Teton Dam Canyon Cluster and the Menan Butte Cluster (specific locations denoted using latitudes and longitudes).

3. To assert the conservation laws for mass, momentum, etc., within an Eulerian system we need to transform the time derivative of an integral over a moving fluid volume into field coordinates; this leads to or requires the Reynolds Transport Theorem.

Please refer to Price, "Lagrangian and Eulerian Representations of Fluid Flow" for additional information about Lagrangian particles 2004.

Due to regional topographic highs such as Menan Butte elevation 5619 ft (1713 m), downstream flooding was pooling (USGS, 1976). Lagrangian particles (gauges) allowed for tracking eddying. Lagrangian particles allow for the analysis of flood velocity data and tracking three-dimensional, time-evolving flow paths. These particles are massless, 3D sensors that are massless and resolved at each time-step.

2.3.2 HEC-RAS Simulations of Downstream Flood from Dam Failure

Modeling of the Teton Dam failure was performed using the unsteady flow option of HEC-RAS 5.0.7, benchmarked through the work of many researchers and practitioners (USACE, 2019).

2.3.3 RAS Mapper- ArcGIS and ArcMap Topography Processing

For comparison purposes of this study, HEC-RAS and GeoClaw used similar inputs. Therefore, the ASCII TetonLarge and TetonLatLong topographies had to be processed into .TIFFs instead of ASCII files. They were processed in ArcGIS 10.8.1 and ArcMap 10.8.1 to output rasters (.TIFFs) readable by HEC-RAS. They also went through a projection conversion from WGS84 to the GCS NAD 1983 State Plane Idaho East FIPS 1101 Feet.

Terrain Development

The first step to parameterizing the historic Teton Reservoir was developing a terrain dataset in HEC-RAS' RAS Mapper. Then, the project's projection was set to the new raster projection for unit: project agreement (A.1). This projection file was created with ArcGIS 10.8.1. Next, a new terrain was dataset was created by layering TetonDamLatLong (10 m) on TetonLarge (30 m) with an elevation of 1/32 (English units). TetonDamLatLong topography has a finer resolution, so it was given a higher priority in the combined Terrain Layer.

2.3.4 Parameterizing the Reservoir

The next step in parameterizing the historic reservoir is the development of a 2D computational mesh. A polygon boundary was drawn for the 2D Teton Reservoir area. The Teton Reservoir (denoted TDRES2D) nominal grid resolution of 200 X 200 ft cells (61 x 61 m cells) were used to build the computational mesh.

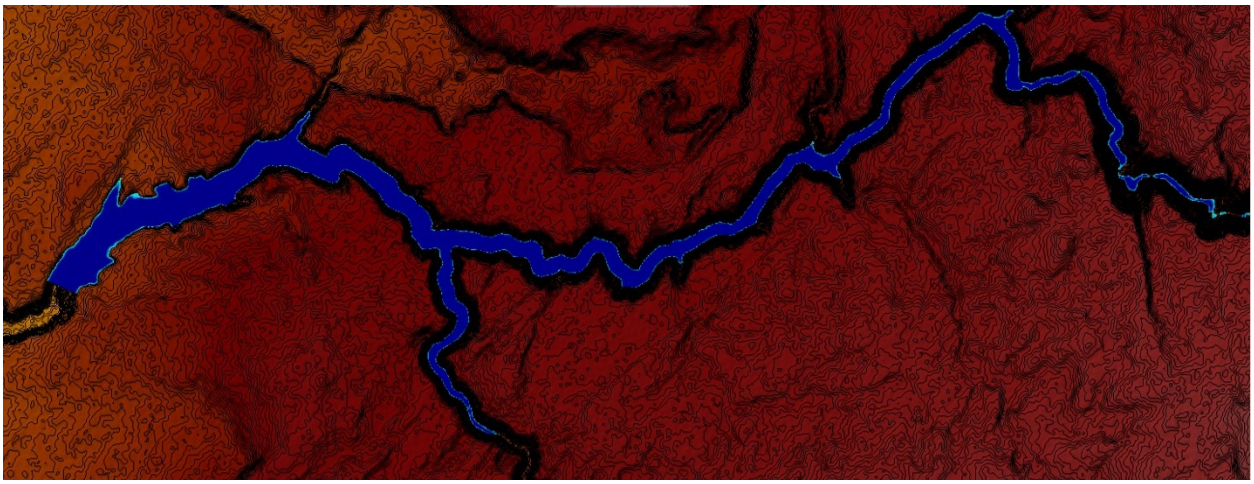

Figure 2.8: Initial HEC-RAS simulation set-up for the parameterized reservoir on TetonDamLatLong.topo with 10 ft (3 m) contour intervals. The blue color denotes the fill of the Teton Reservoir prior to dam breach on 5 June 1976.

2.3.5 Parameterizing the 2D Downstream Flow Area

Similarly, the 2D downstream flow area was drawn in the RAS Mapper geometry editor. With each run, the 2D downstream flow area was refined to reflect the computational area where flow occurred – improving computational efficiency. The final 2D downstream flow area for both the instantaneous HEC-RAS and the time-dependent HEC-RAS models utilized a uniform Manning's coefficient of 0.06 to have similar inputs to GeoClaw (A.9). The sensitivity analysis for this study focuses on the importance of Manning's coefficient. The base of the downstream flow area (2D-DSTREAM) fed into a boundary condition line (BC Line) where the water could exit the simulation.

Additionally, two break-lines were inserted into the simulation to force a cell edge at two important lateral features, differences in elevation (A.15). Through break-lines, we better simulate water flow over cells. The first break-line was within the Teton

Dam canyon downstream of the Teton Dam. Break-line 2 was inserted approximately from (43.980156,-111.581250) to (43.901069, -111.651652).

2.3.6 Geometry Editor

The two 2D Flow Area elements (TDRES2D and TD-DSTREAM) are connected with a storage area 2D connector (SA/2D), which formed the dam as a weir/embankment (A.11, A.12). For the instantaneous dam failure, the dam was parameterized in the geometry editor by modeling the weir to fit the terrain. Therefore, both GeoClaw and HEC-RAS would simulate the dam failure over on the same topography. The Teton Dam reservoir elevation was parameterized at an initial elevation of 5305.3 ft (1617.1 m).

In contrast, for the time-dependent dam failure, the dam was also parameterized in the geometry editor. The dam structure was first built using the historic dam height of 5335.6 ft (1626.3 m). With the 'terrain elevation table' tool, these values were manipulated in Excel to output a table of elevations more like the historic Teton Dam. A logical statement was used to create the new table (in ft):

IF(ELEVATION DATA CELL¡5335.6, 5335.6, ELEVATION DATA CELL)

Then, using the Breach (plan data) section of the SA/2D connector, historic values were implemented to match historical literature values and fit the terrain (A.13). The best fit was identified as having a Center Station of 930 ft (283 m), a final bottom width of 180 ft (55 m), and a final bottom elevation of 5081 ft (1548.7 m). The left-side slope was identified as 1.8, and the right-side slope was 1.9. The breach weir coefficient is 2.6, the breach formation time is 0.5, and the failure mode was 0.5. For further time-dependent dam failure parameterization, the piping coefficient was 0.5 (Reclamation, 1976), and the initial piping elevation from historical literature

(first spot of seepage) was 5238.6 ft (1596.7 m) (Reclamation, 1976). The start date and time of the failure to achieve a maximum breach at 11:57 was 05JUN1976 and a start time of 11:30 AM. A sine wave breach progression was used to depict the rapid progression of the breach (A.14).

2.3.7 Unsteady-Flow Model and Analysis Unsteady Flow Plan

Unsteady Flow Model

The instantaneous dam failure unsteady flow plan requires first picking an appropriate grid size and computational time step. The Teton Dam 2D flow model uses a single elevation at each cell and cell face (standard structured grid-based model). 2D-DSTREAM geometry was constructed to ensure each cell's face captures the high point of barriers to flow. The first models were constructed using the Diffusion Wave equations, and then once they were stable models, they were moved to the complete Saint Venant equations, which means that larger time steps can be used with the Diffusion Wave equations than can be used with the Full Saint Venant equations, and still get numerically stable and accurate solutions.

Unsteady Flow Analysis Plan

For the instantaneous dam failure plan, the simulation time starts at 11:57 on 5 June 1976 - signifying the time of dam breach (Reclamation, 1976) and runs for simulated time 12 hours and 43 minutes. The computational interval was chosen at 30 seconds. The initial parameters 2.9 demonstrate the differences and similarities in the unsteady flow simulation runs. Besides the differing geometry files, the primary difference in the two analysis runs was the simulation start times. As the time-dependent dam failure required the sine wave initiation and the breach lasted

0.5 hours, the simulation begins before the dam breach (10:00) and runs until 0:01 6 June 1976.

HEC-RAS & GeoClaw Instantaneous Dam Failure		HEC-RAS Time Dependent Dam Failure	
Teton Dam Reservoir Elevation	5305.3 ft	Teton Dam Reservoir Elevation	5305.3 ft
Downstream Area Elevation	4300 ft	Downstream Area Elevation	4300 ft
Date and Time Simulation	06 05 1976 11:57 AM	Date and Time Simulation	06 05 1976 11:57 AM
Simulation Duration	11:57 – 24:00	Simulation Duration	11:00 – 24:00

Figure 2.9: Parameterization of the time-dependent and instantaneous dam failures in HEC-RAS.

CHAPTER 3:

RESULTS

3.1 GeoClaw and HEC-RAS Instantaneous Dam Breach Model Results

The ability to quantify, forecast, and calculate the downstream consequences of dam failure is imperative for protecting communities downstream of dams. We compare all historic inundation depths against numerical simulations performed using our GeoClaw numerical dam model.

3.2 Results of GeoClaw and HEC-RAS Models

Results are presented in three sections. The first section focuses on stationary gauge results beginning upstream at the Teton Dam site and moving downstream until Rexburg 25 km downstream. Stationary gauge outputs from GeoClaw can be found in the appendix (A.3,A.4, A.5, A.6, A.7, A.8). The second section focuses on the lateral extent of flooding. The third section focuses on Lagrangian gauge components in GeoClaw and results.

3.2.1 GeoClaw and HEC-RAS Instantaneous Dam Failure Results

The ability to quantify, forecast, and calculate the downstream consequences of dam failure is crucial for protecting communities downstream of dams.

We compare all historic inundation depths (maximum) against numerical simulations performed using our GeoClaw numerical dam model. The results focus on five of the GeoClaw (3.1) and HEC-RAS (3.2) stationary gauges, which logged historic arrival times (hrs) and maximum flow depth (m) of the flood during the model's simulation time. The gauge results are presented below in sequential order moving from the dam progressively downstream: (i) Teton Dam Canyon gauge, (ii) Teton Dam Canyon Mouth gauge, (iii) Wilford gauge, (iv) Sugar City gauge, and the (v) Rexburg gauge. The sensitivity analyses use results from three profile lines that logged flow and flood wave arrival times: (a) Sugar City, (b) Rexburg, and (c) Menan Butte Butte.

Teton Dam Canyon Gauge

The GeoClaw Teton Dam Canyon gauge showed a 24.9 ft (7.6 m) maximum depth flood wave, averaging to 23.95 ft (7.3 m), propagating down the canyon (A.3). As GeoClaw models an instantaneous dam breach, the inundation flood wave arrival time for the GeoClaw Teton Dam Canyon gauge occurs during the second time step – almost immediately at 12:05. In comparison, photographs at the time of failure at the location of the GeoClaw Teton Dam Canyon gauge demonstrate a maximum flood wave depth of about 49 ft (15 m) and arrival times at 12:05 Reclamation (1976). The HEC-RAS Teton Dam Canyon Gauge shows 135.5 ft (41.3 m)

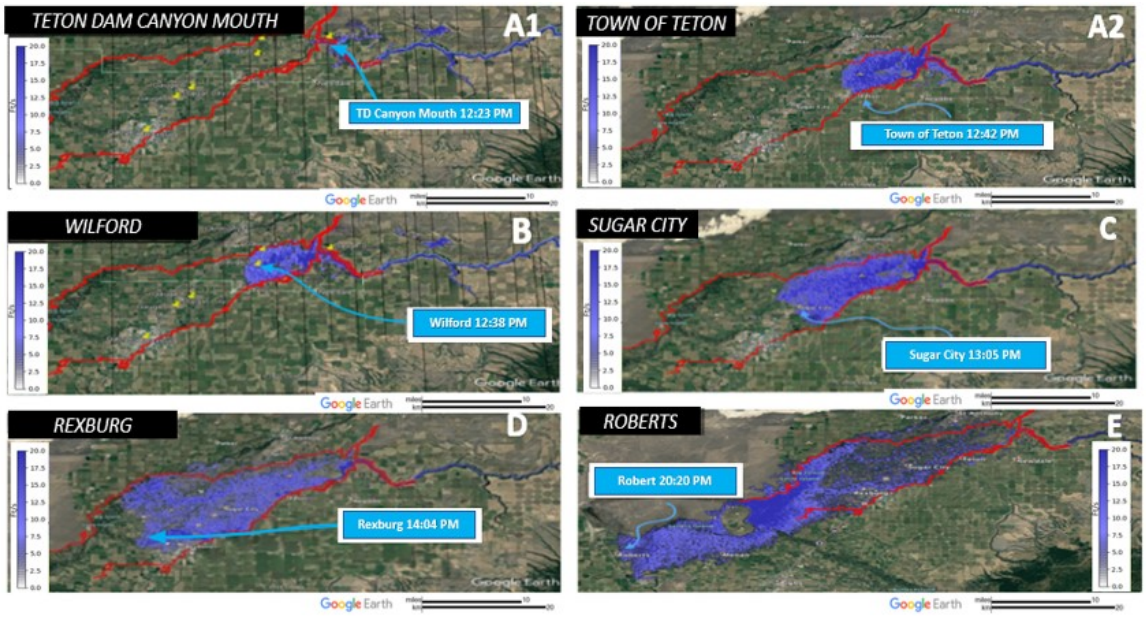

Figure 3.1: GeoClaw Results of lateral extent inundation. A1 - Teton Dam Canyon Mouth. A2 - Town of Teton (not a gauge). B – Wilford Gauge. C – Sugar City. D – Rexburg. E – Roberts (not a gauge). Red outline = historic outline.

maximum depth flood wave, within the Teton Canyon. The flood wave arrives at the HEC-RAS gauge at 11:59, just two minutes following the instantaneous dam breach at 11:57 Reclamation (1976).

Teton Dam Canyon Mouth Gauge

Next downstream, the GeoClaw Teton Dam Canyon Mouth gauge records flood wave arrival time five minutes later at 12:10 (**??**). The GeoClaw gauge registers a maximum flood wave depth of 6.89 ft (2.1 m) inundation, not agreeing with historical values of 38.7 ft - 40 ft (11.8 m- 12.2 m) Reclamation (1976). Then, as the flood laterally spread out of the canyon, it does not flood the town of Teton, agreeing with the lateral extent of the historic flood. However, the historic depths are greater than those modeled in GeoClaw by 30.2 ft (9.2 m). For the HEC-RAS Teton Dam Canyon Mouth Gauge, the maximum recorded depth was 67.6 ft (20.6 m), 27.9 ft (8.5 m) greater than historical values Reclamation (1976). The HEC-RAS gauge logged a flood wave arrival time of 12:06.

Wilford Gauge

At 12:38, when the wave is progressing downstream, the GeoClaw Wilford gauge displays a depth of 8.9 ft (2.7 m) (**??**). Historical literature values show flood waves reaching Wilford at approximately 12:45 with 10.2 ft - 15.1 ft (3.1- 4.6 m) inundation depth Reclamation (1976). The HEC-RAS model Wilford gauge displays maximum inundation depth of 23.6 ft (7.2 m) overestimating the 10.2 ft - 15.1 ft (3.1- 4.6 m) in historical data by about 8.5 meter. Additionally, HEC-RAS had an arrival time at 12:34.

Sugar City Gauge

The GeoClaw Sugar City gauge showed a flood wave arrival time at 13:05 (**??**). The historical literature value for arrival time was 13:30, and flood depth was 10.2 ft (3.1 m) Reclamation (1976). The depth, as displayed in the GeoClaw gauge, is 3.9 ft (1.2 m). The HEC-RAS Sugar City gauge registered a flood wave arrival time at 14:05 Reclamation (1976) and a maximum depth of 11.2 ft (3.4 m).

Rexburg Gauge

The GeoClaw Rexburg gauge demonstrated model values between 3.1 - 3.9 ft (1.2-1.5 m); historical depths were 7.87 ft (2.4 m) Reclamation (1976). The Rexburg GeoClaw gauge logs an arrival time at 14:30, and the historic arrival time is 14:30 Reclamation (1976). The HEC-RAS Rexburg gauge shows an arrival time of 16:25, an hour and 55 minute difference from historical values A.8. The gauge also logs a maximum depth of 112 ft (34 m).

Lateral Extent of Modeled Floods and Computational Costs

The other evaluation principle for the comparison criterion for GeoClaw was determining the lateral flood extent. The GeoClaw model showcased a flood area covered 121 mi^2 (313 km^2) which is within $\pm$ 31 mi^2 (80 km^2) of the historic inundation extent of 130 mi^2 (337 km^2) for the time simulated Reclamation (1976). In comparison, the HEC-RAS model demonstrated a flood area of 174 mi^2 (451 km^2), which is also within $\pm$ 31 mi^2 (80 km^2) of the historical 130 mi^2 (337 km^2) Reclamation (1976).

GeoClaw computational time for runs on the R2 compute cluster, installed at Boise

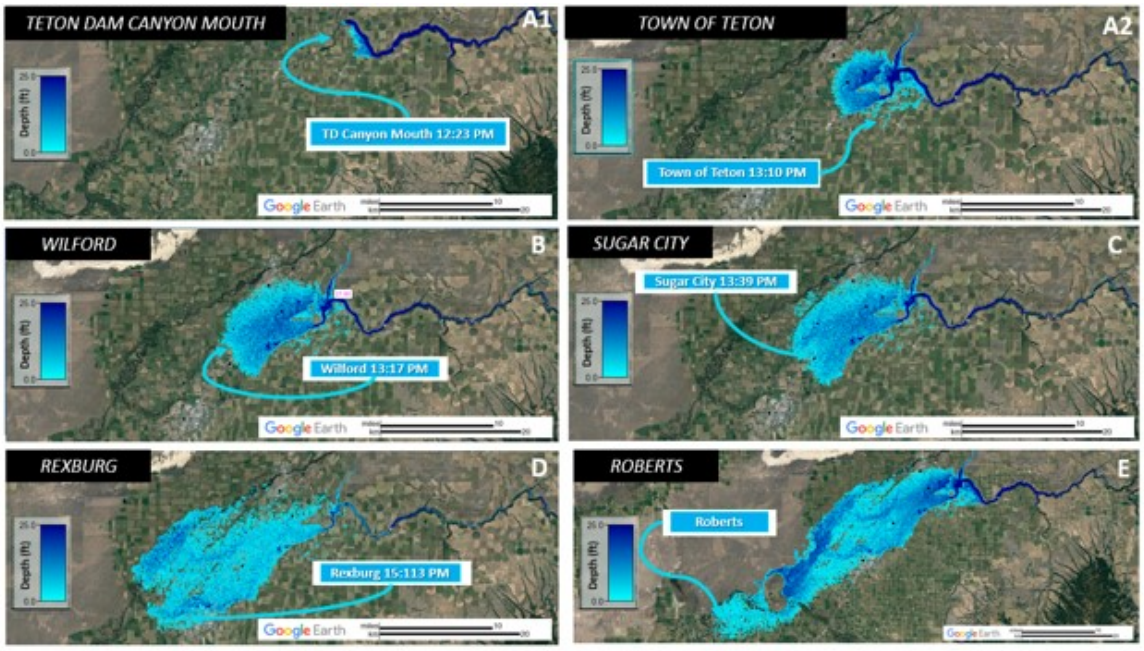

Figure 3.2: HEC-RAS Results of lateral extent inundation. A1 - Teton Dam Canyon Mouth. A2 - Town of Teton (not a gauge). B – Wilford Gauge. C – Sugar City. D – Rexburg. E – Roberts (not a gauge).

State University, is 17 minutes processing time and 15 minutes for plotting (3.3). For HEC-RAS the base model run time was 31 minutes, which includes both run and plot time. Therefore, GeoClaw and HEC-RAS have similar computational wall clock times, 32 minutes compared with 31 minutes. The GeoClaw model ran on 16 OpenMP threads on a single node of the R2 super compute cluster Boise State Research Computing (2017). The computational budget of the HEC-RAS Teton Dam base model included 28 cores and 28 threads on one node. HEC-RAS used a desktop for runs; Intel Xeon E5-2680 v4 14 core 2.4GHz (x2).

Comparison Parameters	GeoClaw Teton Dam Model		HEC-RAS Teton Dam Base Model (Instantaneous Breach)	
Model Run Time	17 minutes*		15 minutes 30 seconds	
Plotting Routine Run Time	15 minutes		0 minutes Outputs plot automatically during run	
Initial Time Step	0.50 seconds		0.50 seconds	
Desired CFL	0.75		0.70	
Maximum CFL	1.00		0.90	
Computational Budget	**Cores:**	8 physical cores and 16 logical cores	**Cores:**	28 cores (máximum)
	CPU:	Intel(R) Core (TM) i9-9900 CPU @3.106 GHz	**CPU:**	Intel Xeon E5-2680 v4 14 core 2.4GHz (x2)
	Threads:	3575 threads average	**Threads:**	28 threads on 1 node

**Model run time in GeoClaw is the duration of processing for setrun.py excluding pre-processing such as making an .exe (compiles Fortran code at the command line) or making a topography (make .topo). Ran on R2 (Boise State Research Computing Department, 2021) with a dev-session (12-hour long CPU session).*

Figure 3.3: Summarizes the computational cost of the HEC-RAS and GeoClaw model simulations.

Lagrangian Gauges Results

This study introduced Lagrangian particles into our depth-averaged flow field to better image the downstream flows for indicating turbulence. Results indicated swirling flow dynamics were observed in the dam failure simulation behind the local topographic high of the domain, Menan Butte (elevation 1713 ft (552 m) MSL); (**??**). As the Lagrangian gauges updated at each time step interval, both clusters demonstrated interesting flow paths within the downstream flood.For example, eddying occurred upstream of Menan Butte and detained six of nine Lagrangian gauges for over 15 minutes. Menan Butte is a large topographic feature, and thus results showed the flow was substantially affected below the Henry's Fork river, where the Snake River begins in Eastern Idaho.

At Henry's Fork, this study noted increased velocities for particles that interacted with the river, as they moved further downstream per time-step than other particles from the same cluster moving over the farmland domain.

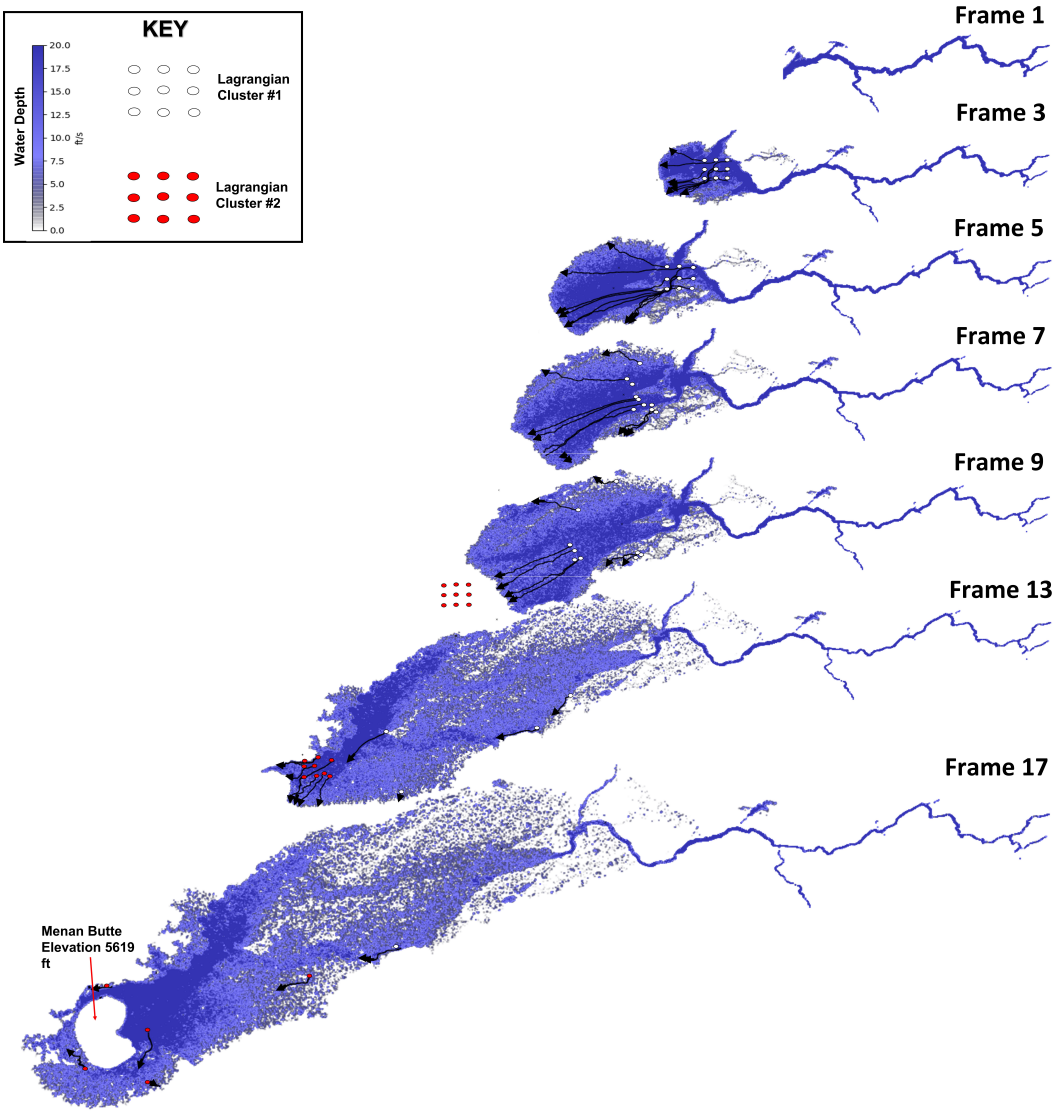

Figure 3.4: Downstream propagation of the Lagrangian gauges (streamlines in black). Results indicate chaotic flow dynamics were observed in the dam failure simulation along with improved run time efficiency due to parallel computing.

3.2.2 HEC-RAS Sensitivity Analysis

This study used four sensitivity analyses to evaluate which parameters in the HEC-RAS model control the numerical solutions. For the HEC-RAS model results,

we analyzed the output flow hydrograph head and tailwaters, the computation log for error percentage, the gauge features for water surface elevation, and three profile lines for flow. The three profile lines, Sugar City, Rexburg, and Menan Butte were chosen based on relative distance downstream and the plethora of historical data. Table 3.1 summarizes the four sensitivity analyses:

1. Manning's roughness coefficient
2. Volume Analysis
3. Instantaneous and Time-Dependent Dam Failure
4. Characteristic Size of the Computational Mesh

Critical trends in the results demonstrate that the reservoir volume controls the peak flow but not the peak flow arrival time. In contrast, the computational mesh controlled peak flow arrival time but had similar peak flows. The Manning's n value was likely overestimated in this study at 0.06, exhibited in the Manning's sensitivity study. Lastly, the instantaneous dam breach assumption was validated as the base model values were identical in peak flow arrival time and comparable in peak flow.

Manning's Roughness Coefficient Sensitivity Analysis

The Manning's n analysis compared roughness values of 0.03-0.07 to determine if the Manning's n value controlled the numerical solution. The base model used a value of 0.06, and all Manning's n values had a slightly different mesh than other models with an expanded domain laterally to allow for natural flow instead of mesh-directed flow. At the Sugar City profile line, the 0.03 Manning's model peak

flow arrived first at 13:18, followed sequentially by progressively smaller Manning's (0.04, 0.05, 0.06, and 0.07); (3.11). The peak flow was largest at the Manning's 0.03 model 1246607 ft^3/s (35300 m^3/s) and smallest for the Manning's 0.07 model 776923 ft^3/s (22000 m^3/s). At the Rexburg profile line, these trends continued as the Manning's 0.03 model peak flow arrived first (14:41), and the Manning's 0.07 model peak flow arrived last (16:25) – a difference of 1 hour and 45 minutes. Historically, the wave arrived in Rexburg at 14:40 Reclamation (1976). The peak flow at the Rexburg profile line was largest for the Manning's 0.03 model 769860 ft^3/s (21800 m^3/s) and lowest for the Manning's 0.07 model 441433 ft^3/s (12500 m^3/s) (3.12). The 0.06 Manning's n model (this study's base model) arrived at 16:25 with a flow of 494405 ft^3/s (14,000 m^3/s). Further downstream, at the Menan Butte profile line, the Manning's 0.03 model peak flow arrives 16:07, and the Manning's 0.07 model peak flow arrives 19:01 3.13. The Manning's 0.03 model peak flow was observed as 278986 ft^3/s (7900 m^3/s), whereas the Manning's 0.07 was recorded as 141259 ft^3/s (4000 m^3/s). The base model, Manning's 0.06, recorded 4600 m^3/s at 19:01. The peak flow between the largest (0.07) and the smallest (0.03) Manning's n models differ by about 23%.

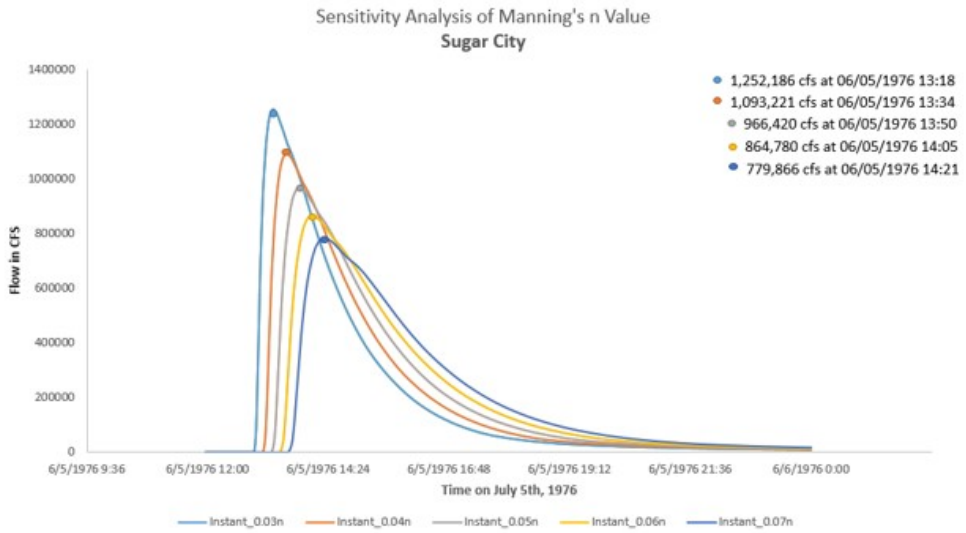

Figure 3.5: Sugar City Profile Line Sensitivity Analysis comparing Manning's n values of 0.03, 0.04, 0.05, 0.06 (base model), and 0.07 – the range of values used by Gundlach & Thomas Bureau of Reclamation in the 1977 simulations 1977.

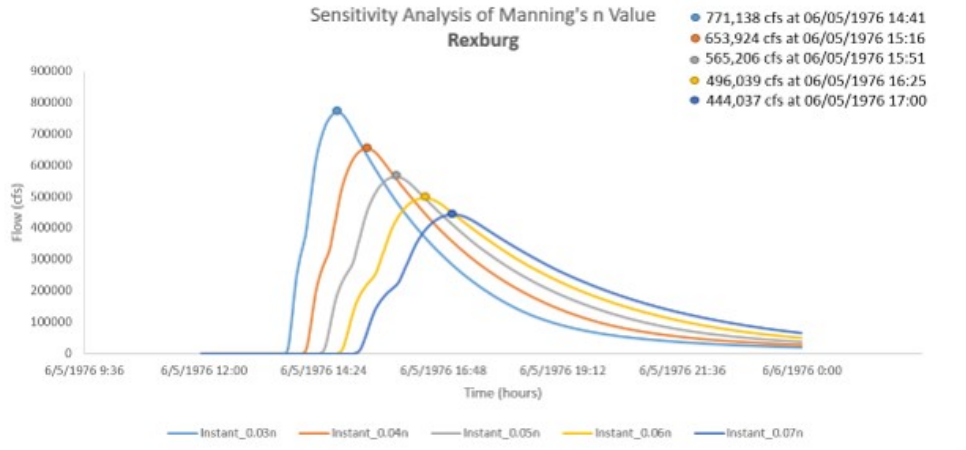

Figure 3.6: Rexburg Profile Line Sensitivity Analysis comparing Manning's n values of 0.03, 0.04, 0.05, 0.06 (base model), and 0.07 – the range of values used by Gundlach & Thomas Bureau of Reclamation in the 1977 simulations 1977.

Volume Sensitivity Analysis

The volume sensitivity analysis compared two volumes. Volume 1 was a volume of 235978 acre-ft (2.29e8 m^3) volume representing the historical Reclamation volume

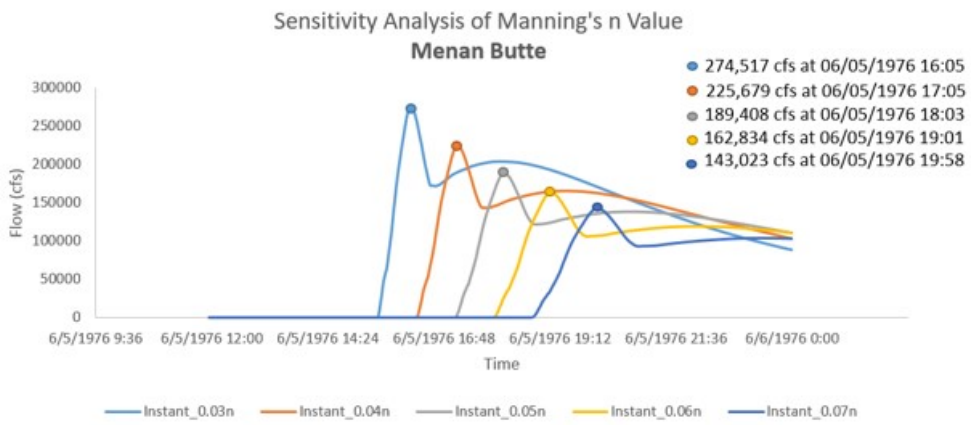

Figure 3.7: . Menan Butte Profile Line Sensitivity Analysis comparing Manning's n values of 0.03, 0.04, 0.05, 0.06 (base model), and 0.07 – the range of values used by Gundlach & Thomas Bureau of Reclamation in the 1977 simulations 1977.

value Reclamation (2000). Volume 2 was the volume created using the initial reservoir depth of 2024 ft (617 m) water surface elevation (WSE; NAVD 88) 213294 acre-ft (2.63e8 m^3) volume model, HEC-RAS Base Model). For the first profile line, Sugar City, the base model (617 m^3/s) arrived at 14:05, similar to the historic volume model (13:58). The peak flow at Sugar City between the two models differs by 113006.9 ft^3/s (3200 m^3/s); historic volume model flow of 974685 ft^3/s (27600 m^3/s) and base model flow of 861677.87 ft^3/s (24400 m^3/s). Further downstream at the Rexburg profile line, the base model arrived at 16:25, and the historic volume model arrived at 16:13. The peak flow rates differed by 84755ft^3/s (2400 m^3/s), with the historic volume model logging the higher flow at 579160.53 ft^3/s (16400 m^3/s). Then, at the third profile line, Menan Butte, the volume analysis demonstrated the historic volume model to arrive first at 18:38, and then the base model arrived at 19:01, a difference of fewer than 25 minutes. The peak flow rate for the models were comparable, with 162448 ft^3/s (4600 m^3/s) (base model) and

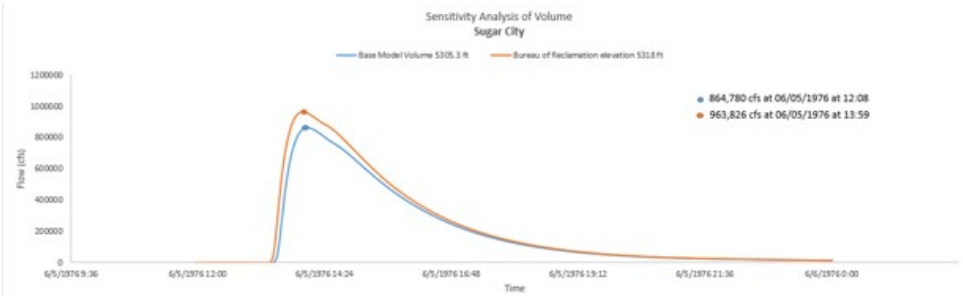

Figure 3.8: Sugar City Profile Line Sensitivity Analysis comparing an initial Teton Reservoir volume of 5305.3 ft (1617 m) to 5318 ft (1621 m) which allows for 324,000 acre-ft volume (3.99 e^8 m^3), like the Bureau of Reclamation measurements (2006).

187168 ft^3/s (5300 m^3/s; historic model), which differ by about 23802 ft^3/s (674 m^3/s).

The peak flow differs between the historic volume model (Volume 1) and Volume 2 by 6% at the Sugar City profile line, 8% at the Rexburg profile line, and 7% at the Menan Butte profile line. The flood wave arrival times differ by about 0.4% at the Sugar City profile line, 0.6% at the Rexburg profile line, and 1% at the Menan Butte profile line.

Characteristic Size of Computational Mesh Analysis

The results of the computational mesh analysis compare the base model mesh (242210 cells; 900 ft x 900 ft (274 x 274 m) - base model mesh) to a mesh with cell sizes increased by 50% (11157 cells; 1300 ft x 1300 ft (411 x 411 m) - lower resolution mesh [LRM]) and a mesh with cell sizes decreased by 50% (980,030 cells; 450 ft x 450 ft (137 x 137 m)-higher resolution mesh [HRM]). The computational cost for the HRM was 4:20:15 hours (15615 seconds), in comparison to the LRM, which processed in 14:03 minutes (843 seconds). The base model computes at 31:13

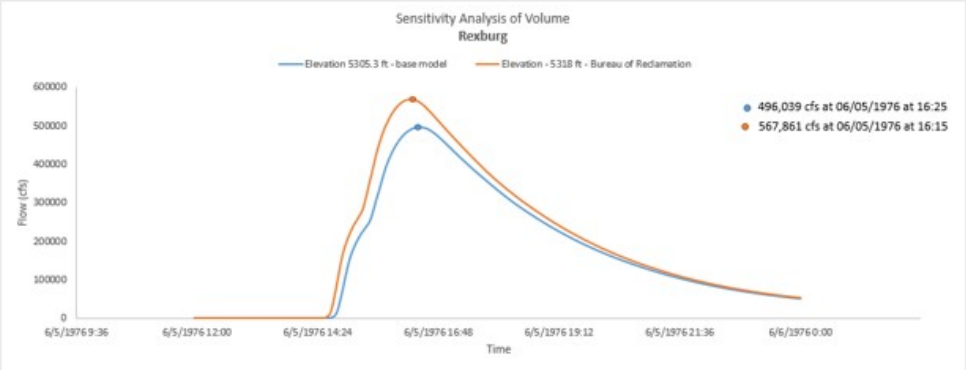

Figure 3.9: Rexburg Profile Line Sensitivity Analysis comparing an initial Teton Reservoir volume of 5305.3 ft (1617 m) to 5318 ft (1621 m) which allows for 324000 acre-ft volume (3.99 e^8 m^3), like the Bureau of Reclamation measurements (2006).

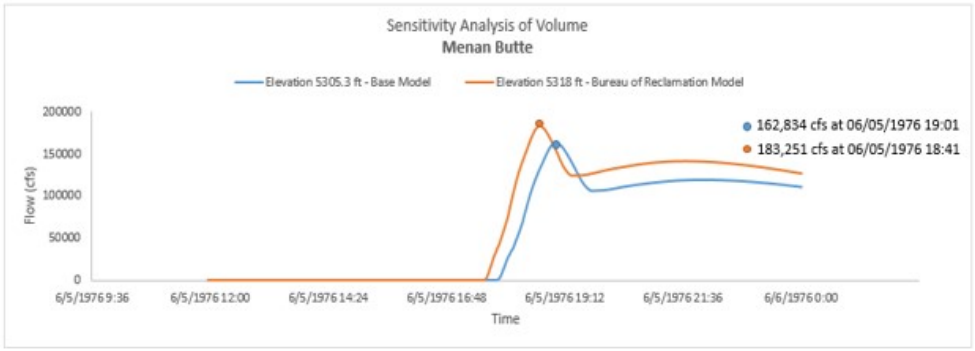

Figure 3.10: Menan Butte Profile Line Sensitivity Analysis comparing an initial Teton Reservoir volume of 5305.3 ft (1617 m) to 5318 ft (1621 m) which allows for 324000 acre-ft volume (3.99 e^8 m^3), like the Bureau of Reclamation measurements (2006).

Table 3.1: HEC-RAS Sensitivity Analyses including the (i) Manning's n models, the (ii) reservoir volume models, the (iii) Characteristic Mesh Size models, and the (iv) instantaneous and time-dependent dam breach models; values presented in SI units (metric). Table includes historic values to reference, sourced from USGS (1976); Reclamation (1976); USGS (2021).

		HEC-RAS Sensitivity Analysis					
		Sugar City profile Line		Rexburg Profile Line		Menan Butte	
		Flow (cubic m)	Arrival Time (hh:mm)	Flow (cubic m)	Arrival Time (hh:mm)	Flow (cubic m)	Arrival Time (hh:mm)
Historical Values		30016 m^3	13:30	None	14:30	2265 m^3	
Manning's n	0.03	35458	13:18	21836	14:41	7850	16:07
	0.04	30957	13:34	18517	15:16	6391	17:05
	0.05	27366	13:50	16005	15:51	5363	18:03
	0.06	24488	14:05	14046	16:25	4611	19:01
	0.07	27745	14:20	12485	17:00	4036	19:39
Reservoir Volume	2.29e8 m^3 Model	24488	14:05	14046	16:25	4611	19:01
	2.63e8 m^3 Model	24488	14:05	14046	16:25	4611	19:01
Computational Mesh Cell Size	Base Model	24488	14:05	14046	16:25	4611	19:01
	Cell Size 50% Incr.	22979	14:14	11111	17:04	3962	20:20
	Cell Size 50% Decr.	22968	14:14	11106	17:04	3963	20:20
Dam Failure Mode	Instantaneous	24488	14:05	14046	16:25	4611	19:01
	Time-Dependent	24488	14:05	14046	16:25	4611	19:01

minutes (1873 seconds). The HRM runs 52% slower than the base model cost, a significant increase in cost.

For the profile line results, the LRM and HRM produced similar results. At the Sugar City profile line the LRM registered 807222 ft^3/s (22858 m^3/s) compared to the HRM 805174 ft^3/s (22800 m^3/s); a difference of 0.1% with both flows lower than the base model flow of 861679 ft^3/s (24400 m^3/s), but only by 3%. At the Sugar City Profile line then, the base model arrives first at 14:05, followed by the LRM and HRM arriving both at 14:14. Both the HRM and LRM log a flow of 391993 ft^3/s (11100 m^3/s), whereas the base model's flow was 11% higher at 494405 ft^3/s (14000 m^3/s). The arrival time of the HRM and LRM were both 17:04, and the base model was 16:25. Further downstream at the Menan Butte profile line, the LRM and HRM arrive again simultaneously (20:20) after the base model (19:01). The LRM and HRM flows were within 1 m^3/s being 141259 ft^3/s (4000 m^3/s respectively); 6% below the base model flow estimate of 162448 ft^3/s (4600 m^3/s).

Instantaneous and Time-Dependent Dam Breach Model Results

For instantaneous breach model versus time-dependent breach model sensitivity analysis, this study assesses the time-dependent scenario and the instantaneous dam breach scenarios in HEC-RAS. Processed flood wave arrival times accounted for the time-dependent breach start time of 10:00 differing by 1:57 hours from the instantaneous breach. At Sugar City profile line, the instantaneous dam breach logs

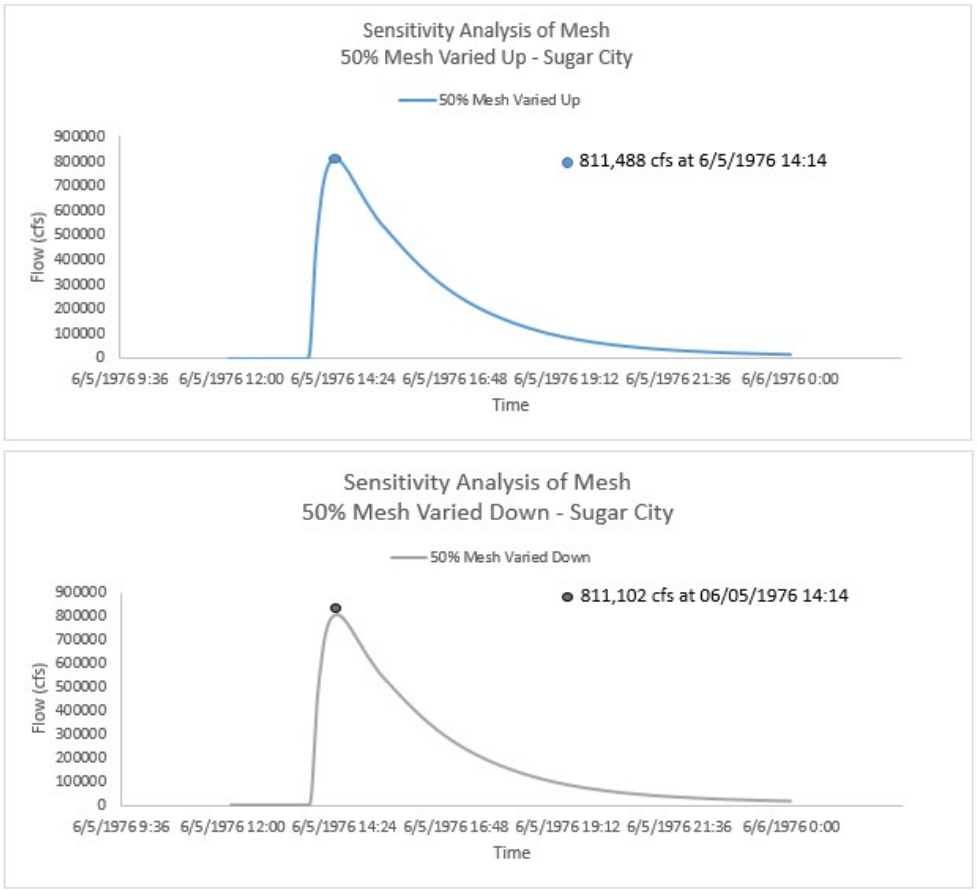

Figure 3.11: Sugar City Profile Line Sensitivity Analysis comparing a finer mesh to a less fine mesh. A. mesh with cell size increased by 50%. B. Mesh with cell size decreased by 50%, increasing the overall number of cells in the mesh.

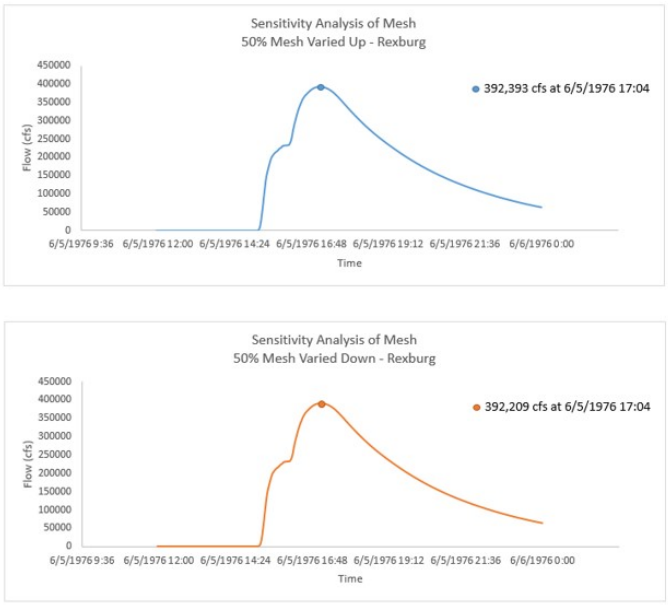

Figure 3.12: Rexburg Profile Line Sensitivity Analysis comparing a finer mesh to a less fine mesh. A. mesh with cell size increased by 50%. B. Mesh with cell size decreased by 50%, increasing the overall number of cells in the mesh.

a flow of 861678 ft^3/s (24400 m^3/s) compared to the time-dependent dam breach value of 8595589 ft^3/s (243400 m^3/s) a difference of 0.2%; both arrive at 14:05. At the Rexburg profile line, both models arrive at 16:25 and log extremely similar values (time-dependent model: 494405 ft^3/s (14000 m^3/s), instantaneous model: 494405 ft^3/s (14000 m^3/s)). Then, at the Menan Butte profile line, both models arrive at 19:01 and log similar flow values. The time-dependent breach logged and the instantaneous breach both logged 162448 ft^3/s (4600 m^3/s). Furthermore, both computational costs were similar varying only by 30 $\pm$2 minutes.

Figure 3.13: Menan Butte Profile Line Sensitivity Analysis comparing a finer mesh to a less fine mesh. A. mesh with cell size increased by 50%. B. Mesh with cell size decreased by 50%, increasing the overall number of cells in the mesh.

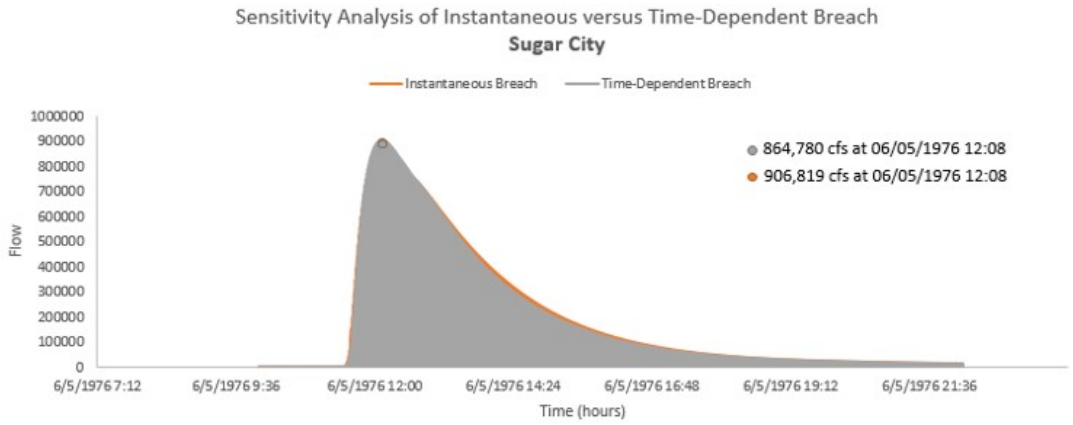

Figure 3.14: Sugar City Profile Line Sensitivity Analysis comparing the instantaneous scenario and the time-dependent breach scenario.

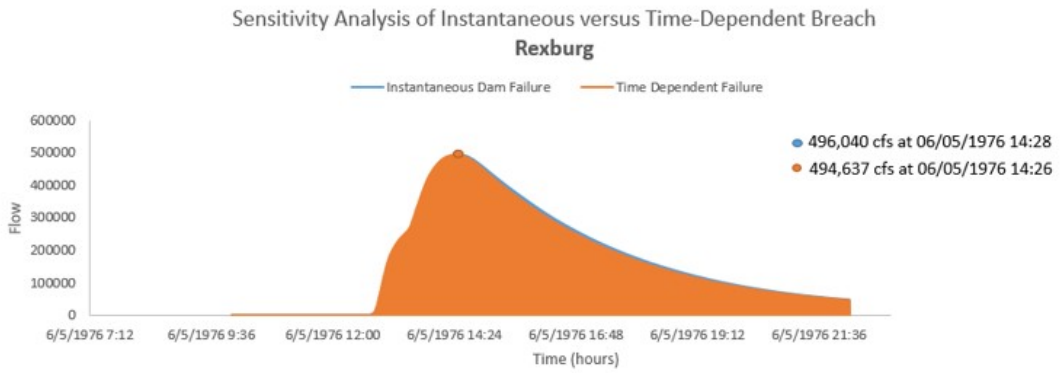

Figure 3.15: Rexburg Profile Line Sensitivity Analysis comparing the instantaneous scenario and the time-dependent breach scenario.

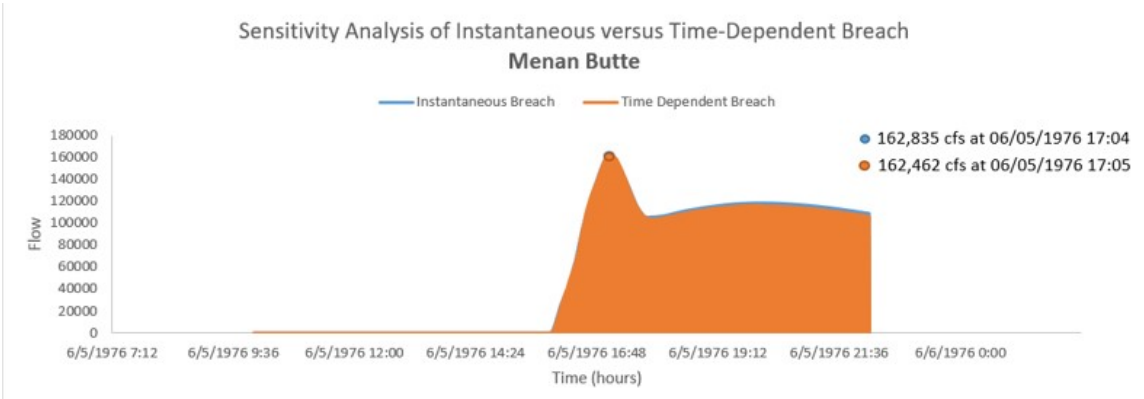

Figure 3.16: Menan Butte Profile Line Sensitivity Analysis comparing the instantaneous scenario and the time-dependent breach scenario.

CHAPTER 4:

DISCUSSION

Dams in the US are aging, and the frequency of dam failures increases with age. Floods are one of the most frequent and costly natural disasters the US faces – including dam failures flooding ASDSO (2021). Dam failures pose a significant threat to human life downstream of the dam. One must first validate and benchmark the software using a historical dam failure assessment to forecast dam failures. One of the guiding questions of the study focused on evaluating GeoClaw for dam failure downstream modeling. The evaluation was based on mathematical formulation controlling flood movement, the capability to predict inundation extent and final flow depth through a numerical method, and the ease of use, performance characteristics, and tools for visualization and post-processing. The second guiding question investigated the model's sensitivity to its parameterization and uncertainty. The stationary gauges used in the two models, HEC-RAS and GeoClaw, allow comparison of flood wave depth and flood wave arrival time. This section discusses the first two gauges: Teton Dam Canyon gauge, Teton Dam Canyon Mouth gauge, and the Wilford gauge. The first GeoClaw gauge, Teton Dam Canyon, showed a flood wave arrival time at 12:05. We consider the GeoClaw Teton Dam Canyon gauge to agree with historical records when evaluating the flood wave arrival time

(12:05 historical arrival time) Reclamation (1976), but not when evaluating by depth as it underestimates the depth by 25 ft (7.62 m). The HEC-RAS model overestimates the flow depth by 17 ft (5.18 m) but agrees with the historical flood arrival time. The GeoClaw Teton Dam Canyon Mouth gauge underestimates the flood depth by 30 ft (9 m).

In contrast, the HEC-RAS model's Teton Dam Canyon Mouth gauge overestimates the depth by about 88.6 ft (27 m), and the flood wave arrival time differs from historical records by over 30 minutes. These differences are significant, and the slow arrival time and overestimation of the depth suggest that Manning's n value of 0.06 is too high in the canyon. However, it is important to note that the Teton Canyon presents the most challenging portion of the flow to model using the SWE. As within the canyon, the extreme vertical accelerations are not well captured by the SWE model.

Continuing the discussion of gauge results with the Wilford, Sugar City, and Rexburg gauges, this study finds GeoClaw and HEC-RAS values similar to historical values. At the Wilford gauge, the GeoClaw model estimated the depth within 3.9 ft (1.2 m) of historical values and the flood arrival time within 15 minutes – which we consider to be excellent agreement. The HEC-RAS model overestimates the flood depth by 15 ft (4.6 m) and demonstrates a flood arrival time difference of 40 minutes which is significant (12:38 historical versus 13:17 model). The GeoClaw Sugar City gauge logged general agreement to the historical literature value arrival time (within 25 minutes) but underestimated the depth by 6 ft (1.8 m). In contrast, the HEC-RAS gauge estimated the flood within 2 ft (0.6 m) of the historical value, and the flood arrival time is within 10 minutes – we consider the

HEC-RAS Sugar City gauge to be in excellent agreement with historical data. Further downstream, the GeoClaw Rexburg gauge also demonstrates inundation agreements with model values within 3 ft (0.9 m) of historical values and the same model arrival time as historical arrival time (14:30). The HEC-RAS Rexburg gauge slightly overestimated historical data; the arrival time differs by over 30 minutes.

Major trends in the results show that the GeoClaw model demonstrates good agreement with historical values for inundation extent, although consistently underestimating depth values. The base model results for HEC-RAS showed agreement with both GeoClaw and with historical data, although consistently overestimating the maximum flow depth and arrival times. For lateral extent evaluation (presented in metric units), the GeoClaw model was 313 km^2 which is within $\pm$ 77.7 km^2 of the historic inundation extent of 337 km^2. However, the HEC-RAS model overestimated the extent which could be related to overestimating the WSE in the reservoir; 450 km^2 HEC-RAS base model compared to the 337 km^2 in historical archives, Reclamation (1976).

In the assessment of the computational cost, both models are comparable with wall clock times between 15-17 minutes. HEC-RAS post-processing requires no additional plotting, whereas GeoClaw requires about 15 minutes of extra processing to produce visualization output. Overall, the results allowed this study to answer the three guiding questions and come across ideas for future work.

4.1 Suitability of GeoClaw

This study investigated if the GeoClaw model was suitable for dam failure downstream modeling of the Teton Dam failure (objectives outlined in 1). We determined the suitability of the GeoClaw software based on its capability to resolve

lateral inundation extent, flood front arrival times, and maximum flood depths. For GeoClaw and HEC-RAS, the calculated area for the lateral extent of the flood largely agrees with historical data. We evaluate the five inundated simulation domains and the modeled time of the six stationary gauges inserted into the GeoClaw simulation for gauge data interpretation. We consider the model in excellent agreement if it predicts the flood wave arrival time within 15 minutes of historical data. We consider the model in good agreement if it predicts the wave within 30 minutes of historical data. Three of the five GeoClaw gauges log flood wave arrival times within ± 7 minutes (Teton Canyon, Teton Canyon Mouth, Wilford -excellent agreement), and all five gauges demonstrate good agreement with historical arrival times. By contrast, the HEC-RAS base model shows three gauges in excellent agreement, one gauge in good agreement, and the Rexburg gauge predicting an arrival time two hours after the historic wave arrived (14:30 compared to 16:25).

For assessing maximum flood depths, this study considered a model in excellent agreement if the depth values were within 5 ft (1.5 m) of historical values. The GeoClaw model is in good agreement if values are within 10 ft (3 m) of historical values. These values also take into account uncertainties in the model, such as ambiguity as to locations where historical values were collected Reclamation (1976). For GeoClaw, two gauges (Wilford and Rexburg) demonstrate excellent agreement with historical data, and Sugar City demonstrates good agreement with historical values. For HEC-RAS, only Sugar City demonstrated excellent agreement, and Rexburg demonstrated good agreement. The Wilford gauge was overpredicted by HEC-RAS 24 ft (7.2 m) compared to the historic 13 ft (4 m). The trends of

GeoClaw show it consistently underestimates the maximum flood depths in the confined canyon area (by 25 ft - 30 ft; 7.6 m - 9.1 m). However, as the modeled GeoClaw flood wave moves downstream out of the canyon, it largely agrees more with maximum flow depths, illustrating perhaps a resolution limitation of GeoClaw in the steep canyon terrain. Potentially, for both HEC-RAS and GeoClaw, using a different roughness coefficient in the canyon could lead to improved and more realistic maximum flow depths.

Other factors considered in model results encompass flood volume, mesh refinement, code efficiency, and pre-processing and post-processing workflows. The pre-processing workflow for GeoClaw involved retrieving metadata in ASCII format and transferring that to the Boise State Compute Cluster R2 Boise State Research Computing (2017). In contrast, HEC-RAS topography processing required changing ASCII data to raster using ArcMap and ArcGIS Pro. When considering mesh refinement, GeoClaw's AMR is advantageous, only resolving where the flood propagates and not requiring an iterative approach to refining the user-defined mesh to improve the downstream mesh. For code and run time efficiency, HEC-RAS and GeoClaw have similar run times. With semi-parallel processing, GeoClaw could improve run times to similar processing and plotting speeds. For example, future work could use the ForestClaw package which could run GeoClaw using distributed computing Calhoun & Burstedde (2017). For the HEC-RAS post-processing workflow, as the model runs, the RAS Mapper window simultaneously updates and stores all results allowing for visualization over the terrain or online map imagery.

4.1.1 What is the importance of breach progression in dam failure modeling?

The importance of a dam breach was assessed by comparing the HEC-RAS time-dependent breach model to the instantaneous breach model. Both models yielded extremely similar results, and the same flood wave arrival times at all three profile lines. The sensitivity analysis required almost identical flows. Therefore, with the similar outputs between the two models, we consider using an instantaneous dam breach estimate rather than parameterizing the historical time-dependent dam breach to be valid.

4.1.2 What is the uncertainty associated with using HEC-RAS for dam failure modeling?

Another objective of this study was to determine the sensitivity of the HEC-RAS model. The results from the sensitivity analyses indicate the volume and the Manning's roughness coefficient were shown to largely control the solution and introduce uncertainty into the model.

For the volume sensitivity analyses, this study compared the historic volume of $2.29e^8$ m^3 Reclamation (2000) to the base model volume of 2.63 e^8 m^3. The results indicated that the peak flow values between the historic and base models were progressively aligned as the flood wave moved downstream and laterally expanded. From Sugar City (flow difference of 113007 ft^3/s (3200 m^3/s)) to Menan Butte (difference of only 84755 ft^3/s (2400 m^3/s)). However, the peak flow rates did show a range, so knowing an accurate reservoir volume is critical to building a reliable dam failure model.

In this study, the Manning's n value also controlled the solution. For instance, the Sugar City profile line logs the 0.04 n flow arriving at 13:34, which is closer to the historical value of 13:30 than the 0.06 n base mode which arrived at 14:05 (difference of 35 minutes). Further downstream, the Rexburg profile line logs the 0.03 n flow arriving at 14:41, close to the historical value of 14:30. However, the base model (0.06 n) arrives at 16:25, nearly 2 hours later – a significant difference. We recommend that future work involves a depth-variable Manning's roughness coefficient or a variable Manning's roughness coefficient throughout the domain, given that the Manning's sensitivity analysis showed that the roughness wholly affects the simulation and computational results.

Although previous studies demonstrated that the mesh could control a dam failure flood solution, we conclude from the mesh sensitivity analysis that the mesh does not control or impact the solution of the Teton Dam flood wave arrival time or flow. With the low relief of the terrain (with Menan Butte and the Teton canyon as the only exceptions), and the fairly high resolution cell-gridding, the mesh does not change the computational result. However, the geometry is a crucial source of potential error in any hydraulic model with uncertainty. For example, having a higher resolution topography 16 ft (5 m) rather than 32 ft (10 m) for the dam's reservoir could improve reservoir volume predictions to be closer to historical values. Additionally, there is an uncertainty associated with the historical depth value, as they were not directly associated with a location (longitude and latitude) when collected in 1976. Therefore, with that data limitation, there is uncertainty associated with the historical values. Future work could include a survey in Eastern Idaho of remaining structures to document known high watermarks to improve this

data limitation. Then, this uncertainty could be eliminated by integrating those locations as stationary gauges.

The HEC-RAS hydrologic model a widely used dam failure modeling software in the US. HEC-RAS in the past has been used to model the Teton Dam failure using the 1D unsteady flow routing (1D SWE equations) to route an inflowing flood hydrograph through a reservoir Land (1980). In this project, we expand on previous research, employing HEC-RAS v.5.0.7 2D unsteady flow routing capabilities (Full Momentum SWE) for comparison to GeoClaw. This study found both HEC-RAS and GeoClaw to produce similar numerical solutions and resultant simulations with numerical gauges depicting maximum flow depths and flood wave arrival times that largely agreed with historical data. With this study and the results, we would recommend using GeoClaw for forecasting or hindcasting downstream flow behavior from dam breach simulations.

4.2 Recommendations for Future Work

4.2.1 Drone Photogrammetry Generated Topographies in Dam Failure Modeling

As some dams are in remote locations where only coarse DEMs exist, drone photogrammetry could be a valuable tool for creating supplemental high-resolution DEMs. We recommend that future work investigate high-resolution topography usage in GeoClaw dam breach modeling, focusing on resolution and efficiency. Initial testing demonstrated that drone photogrammetry-generated topography could be uploaded into the HEC-RAS's RAS Mapper as a terrain in GeoTiff format. Through uploading the three raster data sets in this study, HEC-RAS can further

import them within a single layer, which can be merged into a single raster. Using HEC-RAS or any ESRI product (ArcMap or ArcGIS Pro), exported combined terrains could be loaded into GeoClaw for a resolution and run-time efficiency-focused study.

4.2.2 Teton Dam GeoClaw Model Manning's Coefficient

This study recommends additional Manning's sensitivity analyses to be performed, comparing uniform Manning's n values which spatially varying Manning's roughness sensitivity analyses and depth-averaged Manning's n. This additional study and analysis would involve an in-depth geomorphological characterization survey of the Teton Canyon, and comparing present-day evidence to historical data to determine the uncertainties of the topographical data. Additionally, to improve uncertainties in this model, we recommend quantifying the geomorphological differences in the canyon from 1976 pre-failure to the present day data as the volume of landslide debris that might be offsetting reservoir fill volume values in this study. Future work could involve simulation of a higher-resolution Teton Canyon (generated from drone photogrammetry as well) which might increase computation times, but could improve downstream canyon values.

4.2.3 Depth-Averaged Debris Modeling of Teton Dam failure

The current GeoClaw model uses the SWEs and Lagrangian particles to track streamlines. The massless Lagrangian particles could be further parameterized with mass, size, drag (function of particle Reynolds number), and buoyancy – the most significant forces acting on fluid objects. Through further parameterization, the user could model debris carried in the dam failure flood wave such as cattle, houses, sediment (sand), and timber. GeoClaw could use model development like

COULWAVE and ComMIT/MOST(NOAA) to simulate buoyant debris. However, research explores the simulation of debris sourced from vegetation, vehicles, or non-buoyant debris (the additional parameterized Lagrangian gauges) such as buildings, sand, and rock. The Teton Dam failure provides an opportunity for future work in this area, which could help forecast dam failure risk and can assess costs as debris removal, improving community resilience.

Open Research

The study used open-source software HEC-RAS USACE (2019) and GeoClaw Clawpack Development Team (2021) for 2D numerical modeling. The Teton Dam models (version used in this paper) are located on GitHub with a (i) READme.md file that includes the metadata and a complete model description, (ii) configuration parameters along with the specific script and workflow which is preserved in the repository, and the (iii) code which can produce the data that supports the summary results, tables and figures Spero, Hannah and Calhoun, Donna and Schubert, Michael (2021). Additionally, this study used the high-performance computing support of the R2 compute cluster (DOI: 10.18122/B2S41H) provided by Boise State University's Research Computing Department Boise State Research Computing (2017).

Data Availability Statement

Both the (i) ASCII topography data used for creating the underlying terrain, and (ii) the GeoClaw and HEC-RAS project files are available at [GitHub: Spero-Hannah/Teton-Dam-Failure-Example] via [DOI: 10.5281/zenodo.586668, persistent identifier link] with [Berkeley Software Distribution (BSD) license]; Spero,

Hannah and Calhoun, Donna and Schubert, Michael (2021). Unmodified topography files can be found on the USGS website USGS (2015).

REFERENCES

Almassri, Belal. 2011. *Numerical Simulation Analysis of Dam Breaks using ISIS & HEC-RAS*. Ph.D. thesis, Palenstine Polytechnic University.

Arcos, Maria, & LeVeque, Randall J. 2015. Validating Velocities in the GeoClaw Tsunami Model Using Observations Near Hawaii from the 2011 Tohoku Tsunami. *Pure and Applied Geophysics*, **172**(3), 849–867.

ASDSO. 2021. *Dam Failures and Incidents*.

Balloffet, Armando, & Scheffler, Michael. 1982. Numerical Analysis of the Teton Dam Failure Flood. *Journal of Hydraulic Research*.

Berger, Marsha, George, David, LeVeque, Randall, & Mandli, Kyle. 2011. The GeoClaw Software for Depth-Averaged Flows with Adaptive Refinement. *Advances in Water Resources*, **34**(9), 1195–1206.

Blanton, J. 1977. Floodplain Inundation Caused by Dam Failure. *In: Proceedings of Dam-Break Flood Routing Model Workshop*.

Boise State Research Computing. 2017. *R2: Dell HPC Intel E5v4 (High Performance Computing Cluster)*.

Brown, R. 1977. A Simulation of the Hydraulic Events During and Following the Teton Dam Failure. *In: Proceedings of Dam-Break Flood Routing Model Workshop*.

Brunner, Gary. 2002. HEC-RAS (River Analysis System). *Pages 3782–3787 of: North American Water and Environment Congress & Destructive Water*. ASCE.

Brunner, Gary. 2016. Benchmarking of the HEC-RAS Two-Dimensional Hydraulic Modeling Capabilities. *US Army Corps of Engineers—Hydrologic Engineering Center*, 1–116.

Brunner, Gary, Piper, Steven, Jensen, Mark, & Chacon, Ben. 2015. Combined 1D and 2D Hydraulic Modeling within HEC-RAS. *Pages 1432–1443 of: World Environmental and Water Resources Congress 2015*.

Calhoun, Donna, & Burstedde, Carsten. 2017. ForestClaw: A Parallel Algorithm for Patch-Based Adaptive Mesh Refinement on a Forest of Quadtrees. *arXiv preprint arXiv:1703.03116*.

Carter, B. 1976. Field Inspection of Shallow Slides on the Teton Reservoir. *Teton Project, Idaho, Reclamation Memorandum from Regional Director, Boise, Idaho, to Director of Design and Construction Engineering and Research Center, Denver, Colorado*.

Chow, Te. 1959. *Open Channel Hydraulics*.

Clawpack Development Team. 2020. *Clawpack (GeoClaw) Software*. Version 5.7.1.

Clawpack Development Team. 2021. *Clawpack v5.8.0 Release Notes*.

Costabile, Pierfranco, Costanzo, Carmelina, Ferraro, Domenico, Macchione, Francesco, & Petaccia, Gabriella. 2020. Performances of the New HEC-RAS Version 5 for 2D Hydrodynamic-Based Rainfall-Runoff Simulations at Basin Scale: Comparison with a State-of-the art Model. *Water*, **12**(9), 2326.

FEMA. 2013. *Living with Dams: Know Your Risk*. "Federal Emergency Management -FEMA P-956 Catalog No. 13052-3".

Fread, D. 1977. The Development and Testing of a Dam-Break Flood Forecasting Model. *In: Proceedings of Dam-Break Flood Routing Model Workshop*.

George, D. 2006. *Finite Volume Methods and Adaptive Refinement for Tsunami Propagation and Inundation*. University of Washington.

George, D. 2008. Augmented Riemann Solvers for the Shallow Water Equations over Variable Topography with Steady States and Inundation. *Journal of Computational Physics*, **227**(6), 3089–3113.

George, D. 2011. Adaptive Finite Volume Methods with Well-Balanced Riemann Solvers for Modeling Floods in Rugged Terrain: Application to the Malpasset Dam-Break Flood (France, 1959). *International Journal for Numerical Methods in Fluids*, **66**(8), 1000–1018.

Godunov, Sergei, & Bohachevsky, I. 1959. Finite Difference Method for Numerical Computation of Discontinuous Solutions of the Equations of Fluid Dynamics. *Matematičeskij sbornik*, **47**(3), 271–306.

González, Frank, LeVeque, Randall, Chamberlain, Paul, Hirai, Bryant, Varkovitzky, Jonathan, & George, David. 2011. Validation of the GeoClaw Model. *In: NTHMP MMS Tsunami Inundation Model Validation Workshop. GeoClaw Tsunami Modeling Group*.

Gundlach, David, & Thomas, William. 1977. *Guidelines for Calculating and Routing a Dam-Break Flood*. Department of Defense, Department of the Army, Corps of Engineers.

Hervouet, Jean-Michel, & Petitjean, Alain. 1999. Malpasset Dam-Break Revisited with Two-Dimensional Computations. *Journal of Hydraulic Research*, **37**(6), 777–788.

Land, Larry. 1980. *Evaluation of Selected Dam-Break Flood-Wave Models by Using Field Data*. US Geological Survey (USGS) Water-Resources Investigations 80-44.

LeVeque, Randall, George, David, & Berger, Marsha. 2011. Tsunami Modelling with Adaptively Refined Finite Volume Methods. *Acta Numerica*, **20**, 211–289.

LLC, Agisoft. 2006. *Agisoft*.

Macchione, F, & Sirangelo, B. 1990. Floods Resulting from Progressively Breached Dams. *Hydrology in Mountainous Regions. II-Artificial Reservoirs; Water and Slopes*, 325–332.

MacInnes, Breanyn, Gusman, Aditya, LeVeque, Randall, & Tanioka, Yuichiro. 2013. Comparison of Earthquake Source Models for the 2011 Tohoku Event Using Tsunami Simulations and Near-Field Observations. *Bulletin of the Seismological Society of America*, **103**(2B), 1256–1274.

Magleby, D. 1981. Post Failure Landslides. *Teton Reservoir, Minidoka Project, Idaho, US Department of the Interior, Water and Power Resources Service, Boise, Idaho*.

Magleby, D.N. 1981. *Post Failure Landslides, Teton Reservoir, Minidoka Project, Idaho, US Department of the Interior, Water and Power Resources Service, Boise, Idaho*.

Mandli, Kyle, & Dawson, Clint. 2014. Adaptive Mesh Refinement for Storm Surge. *Ocean Modelling*, **75**, 36–50.

Mandli, Kyle, Ahmadia, Aron, Berger, Marsha, Calhoun, Donna, George, David, Hadjimichael, Yiannis, Ketcheson, David, Lemoine, Grady, & LeVeque, Randall. 2016. Clawpack: Building an Open Source Ecosystem for Solving Hyperbolic PDEs. *PeerJ Computer Science*, **2**, 68.

Patel, Dhruvesh P, Ramirez, Jorge A, Srivastava, Prashant K, Bray, Michaela, & Han, Dawei. 2017. Assessment of Flood Inundation Mapping of Surat City by Coupled 1D/2D Hydrodynamic Modeling: A Case Application of the New HEC-RAS 5. *Natural Hazards*, **89**(1), 93–130.

Pierce, Kenneth, Morgan, Lisa, Link, P, Kuntz, M, & Platt, L. 1992. The Track of the Yellowstone Hot Spot: Volcanism, Faulting, and Uplift. *Regional Geology of Eastern Idaho and Western Wyoming: Geological Society of America Memoir*, **179**(322), 1–53.

Price, James. 2004. Topics in Fluid Dynamics: Dimensional Analysis, the Coriolis force, and Lagrangian and Eulerian Representations. *MIT DSpace (Digital Repository)*.

Reclamation. 1976. *Report to the US Department of the Interior and State of Idaho on Failure of Teton Dam*.

Reclamation. 2000. *Geomorphology and River Hydraulics of the Teton River Upstream of Teton Dam, Teton River, Idaho*. US Department of the Interior, Bureau of Reclamation.

Reclamation. 2006. *Teton River Resource Management Plan*.

Reclamation. 2008. *The Teton Dam Failure - An Effective Warning and Evacuation*.

Reclamation. 2015. *Drone Photogrammetry Data. Reach 01 Containing Teton Dam. Bureau of Reclamation under the Department of the Interior*.

Schuster, Robert, & Embree, G. 1980. Landslides Caused by Rapid Draining of Teton Reservoir, Idaho. *In: Proceedings of the Eighteenth Annual Engineering Geology and Soils Engineering Symposium, held at the Red Lion Inn, Boise, Idaho*.

Smith, Curtis, Prescott, Steven, Ryan, Emerald, Calhoun, Donna, Sampath, Ramprasad, Anderson, Danielle, & Casteneda, Cody. 2015. *Flooding Capability for River-Based Scenarios*. Tech. rept. Idaho National Lab.(INL), Idaho Falls, Idaho, US.

Snyder, F. 1977. Floods from Breaching of Dams. *In: Proceedings of Dam-Break Flood Routing Model Workshop*.

Spero, Hannah, Miller, Kenny, Vazquez Lopez, Iker, Joshaghani, Rezvan, Cutchin, Steven, Calhoun, Donna, & Enterkine, Josh. 2021. In Revisions. Communicating Dam Failure Hazards to Society Through a Virtual Reality Environment of the Teton Dam Failure. *International Journal of Digital Earth*.

Spero, Hannah and Calhoun, Donna. 2020. Modeling the Downstream Consequences of the 1976 Teton Dam Failure and Resulting Flood by Validating the GeoClaw Software with Historical Data.

Spero, Hannah and Calhoun, Donna and Schubert, Michael. 2021. *Teton Dam Repository v.1.0.1.*

Stanford University. 2018. *National Performance of Dams Program.* Department of Civil & Environmental Engineering.

Thomas, W. 1977. Calculating and Routing the Teton Dam-Break Flood. *In: United States Water Resources Council.*

Turzewski, Michael, Huntington, Katharine, & LeVeque, Randall. 2019. The Geomorphic Impact of Outburst Floods: Integrating Observations and Numerical Simulations of the 2000 Yigong Flood, Eastern Himalaya. *Journal of Geophysical Research: Earth Surface*, **124**(5), 1056–1079.

USACE. 2019.

USACE. 2021. *HEC-HMS Validation Guide.*

USGS. 1976. *Teton Dam Flood of June 1976.* Map 1:24,000 scale.

USGS. 2015. *United States Geological Survey of the U.S. Department of the Interior. Eastern Idaho Topography: U.S. Geological Survey database at 10m and 30 m resolution.*

USGS. 2021. *United States Geological Survey Gage 13056500 Henry's Fork Near Rexburg, Idaho.*

Valiani, Alessandro, Caleffi, Valerio, & Zanni, Andrea. 2002. Case Study: Malpasset Dam-Break Simulation Using a Two-Dimensional Finite Volume Method. *Journal of Hydraulic Engineering*, **128**(5), 460–472.

APPENDIX A:

APPENDIX 1

Description	NGVD 29 (1976)	NAVD 88 (Present Day)
Elevation of Reservoir at Time of Failure	5301.7ft	5305.3 ft
Maximum WSE (Water Surface Elevation) of Full Reservoir Capacity	5324.3ft	5327.9 ft
Elevation of Reservoir Base	5060 ft	5063.6 ft
Elevation of Reservoir Crest	5332 ft	5335.6 ft

Figure A.1: Vertical Datum Conversions for important dam parameter values. Values for NGVD 29 below are from the US Department of Interior, Bureau of Reclamation, December report, as this is the primary source (Reclamation, 1976)

Topography	Teton LatLong
4180	Number of grid points in x: ncols
1464	Number of grid points in y: nrows
-112.390734400000	xlow: xllcorner
43.581746970335	ylow: yllcorner
-111.2298244003	xhigh: xurcorner, using 0.000277729665 csize
44.742936967335	yhigh: yurcorner, , using 0.000277729665 csize
4849.081	Elevation low
9020	Elevation high #piney peak
30.0000	dx
30.0000	dy
Topography	**Teton Large**
3996	Number of grid points in x: ncols
2988	Number of grid points in y: nrows
-112.360138888891	xlow: xllcorner
43.170138888889	ylow: yllcorner
-111.250138888	xhigh: xurcorner, using 0.000277777778 csize
44.000138889554	yhigh: yurcorner, using 0.000277777778 csize
4472	Elevation low
9020	Elevation high #piney peak
30.0000	dx
30.0000	dy

Figure A.2: Metadata and descriptions of TetonDamLatLong and $\mathbf{Teton}_{L}argetopographies(WGS84)$.

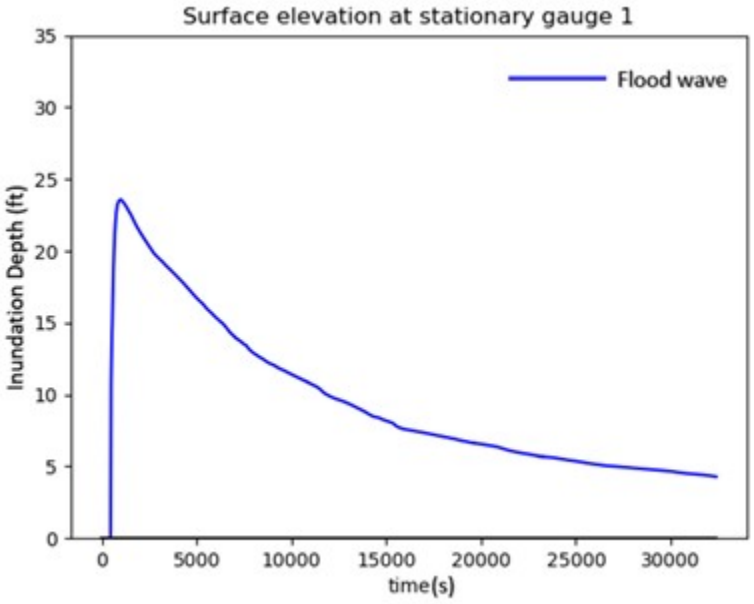

Figure A.3: Stationary Gauge 1 Teton Dam Canyon.

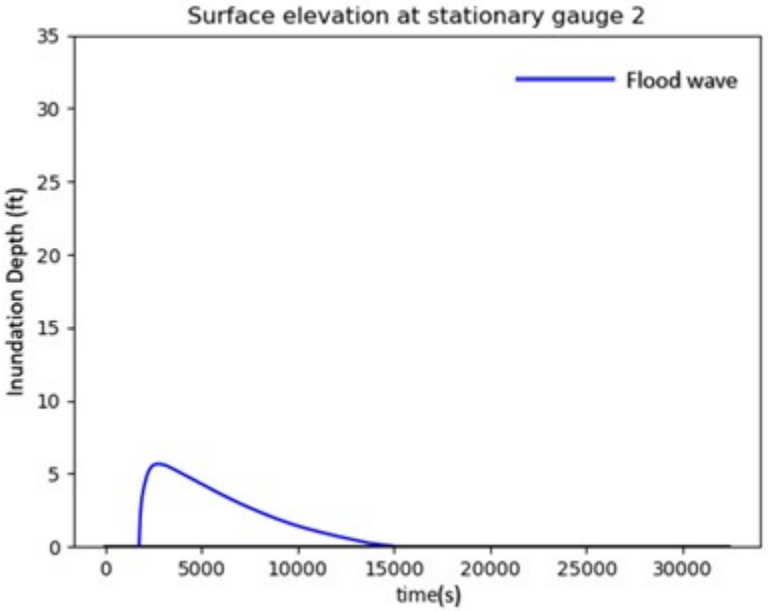

Figure A.4: Stationary Gauge 2 Teton Dam Canyon Mouth.

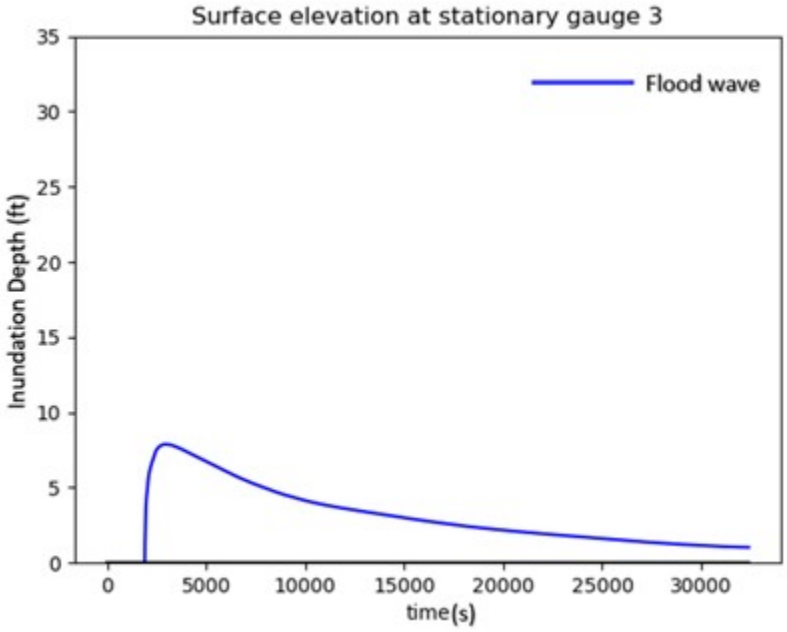

Figure A.5: Stationary Gauge 3 Wilford.

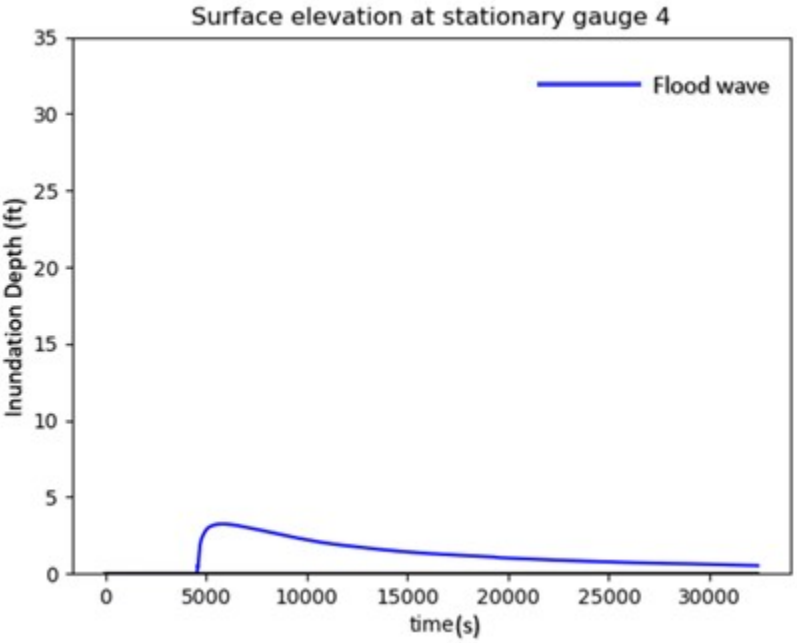

Figure A.6: Stationary Gauge 4 Sugar City.

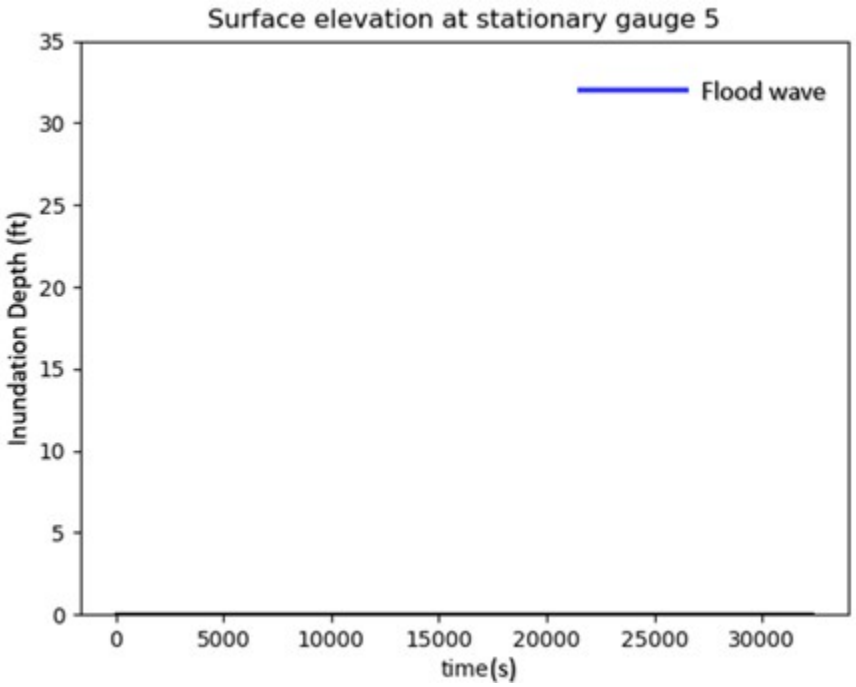

Figure A.7: Stationary Gauge 5 Blackfoot. The flood did not reach Blackfoot within the 11:57-24:00 simulation duration (05 June 1976).

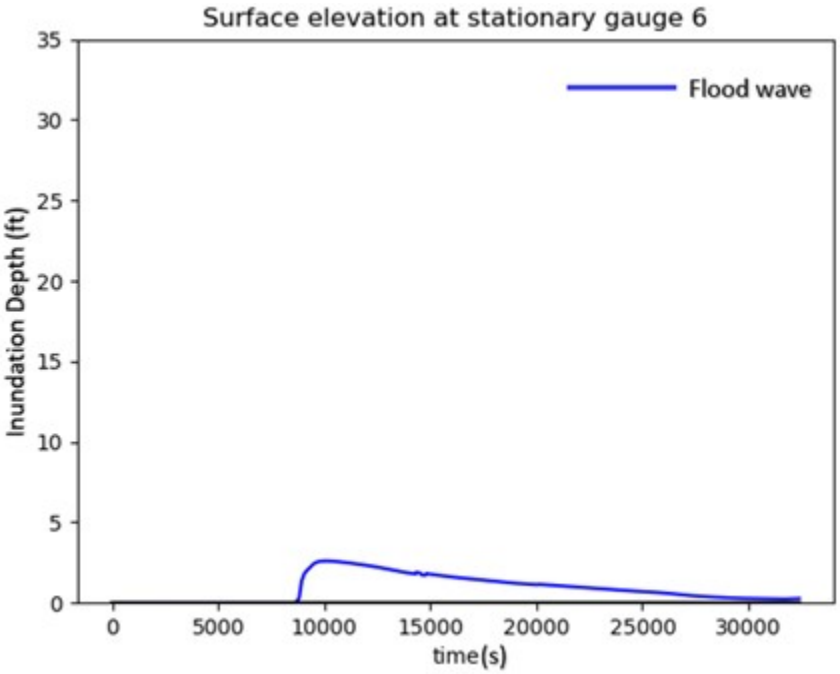

Figure A.8: Stationary Gauge 6 Rexburg.

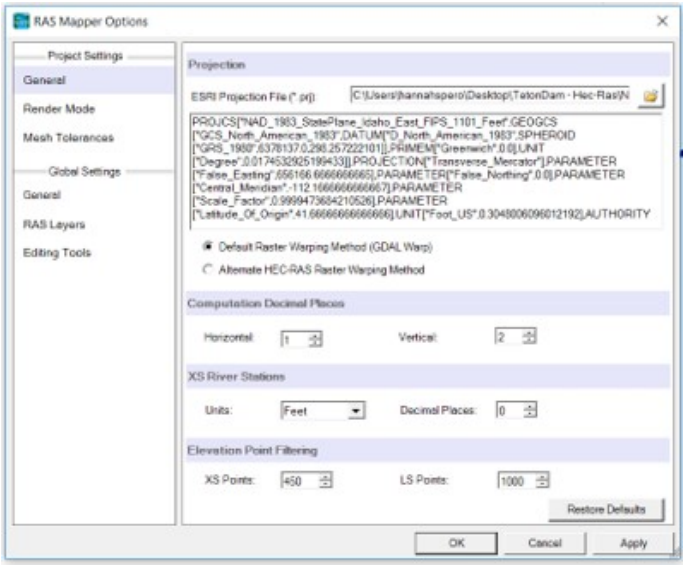

Figure A.9: Editor to set the RAS Mapper project's spatial reference system (coordinate system). Parameterized using an existing ".prj" file (ESRI projection file).

Figure A.10: 2D Teton Reservoir flow area constructed using dx=200 ft, dy=200 ft. Labeled TDRES2D.

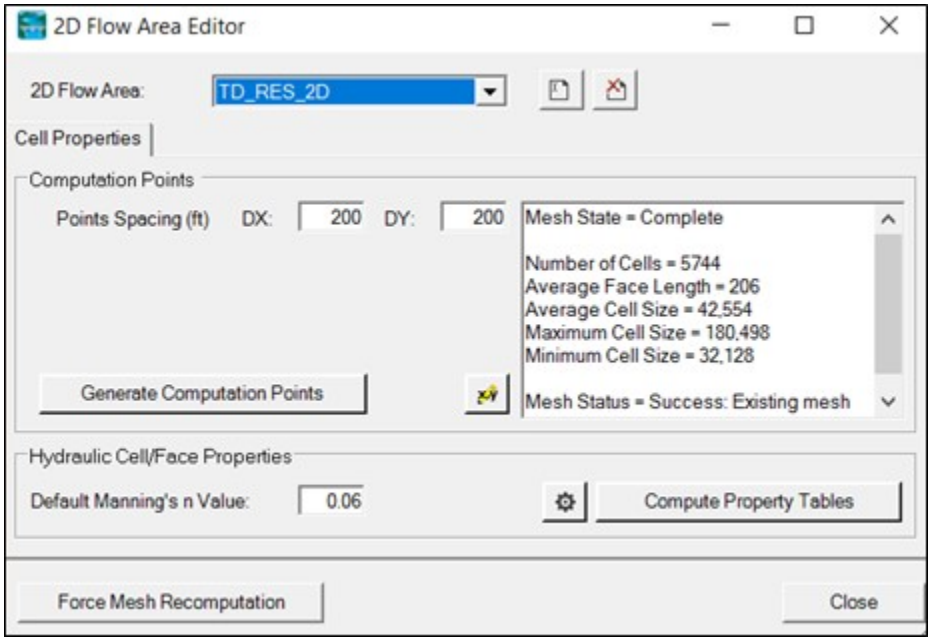

Figure A.11: 2D Flow Area Mesh Generation Editor – Teton Reservoir.

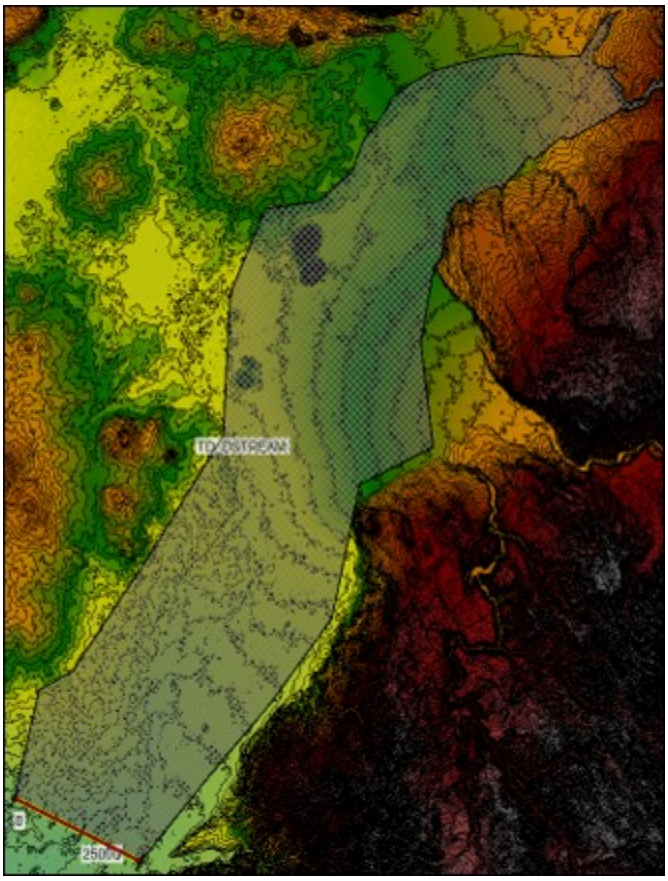

Figure A.12: RAS Mapper 2D downstream area with break line (bottom left) displayed).

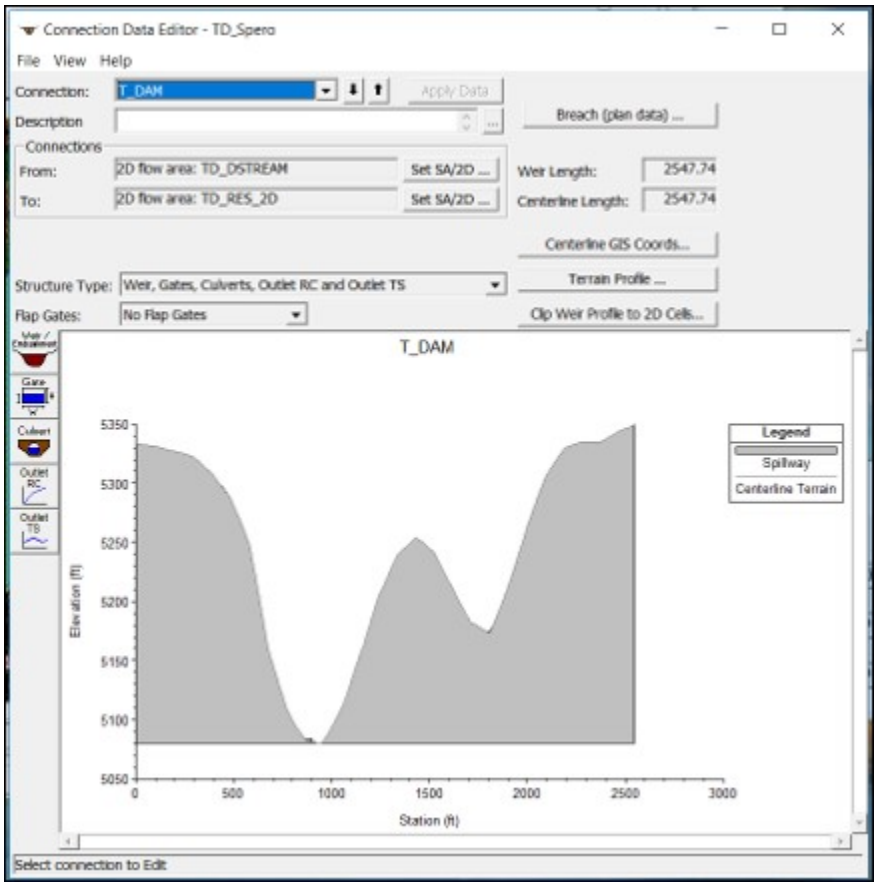

Figure A.13: Clipped weir to 2D cells fitting the terrain profile.

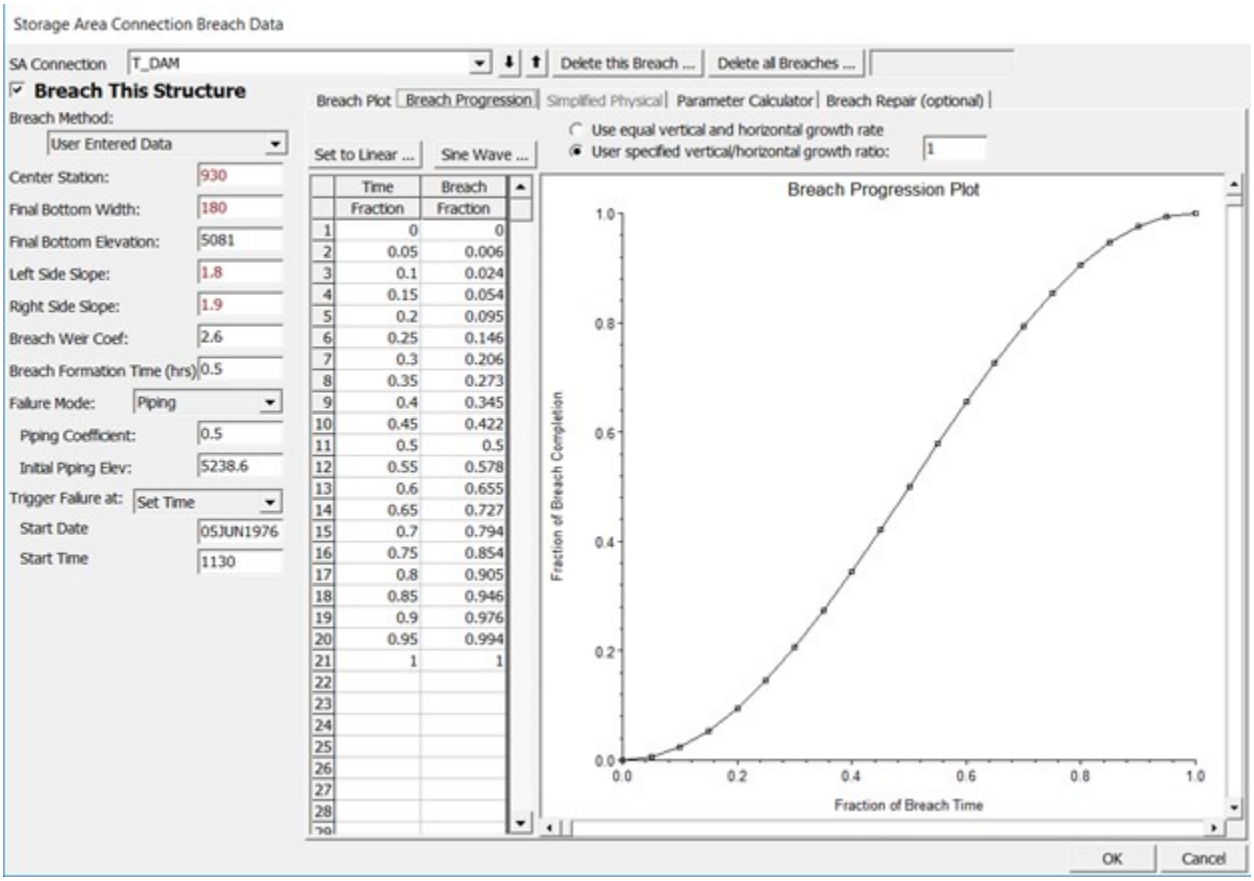

Figure A.14: Breach data editor, with the breach progression of the Teton Dam using the sine function.

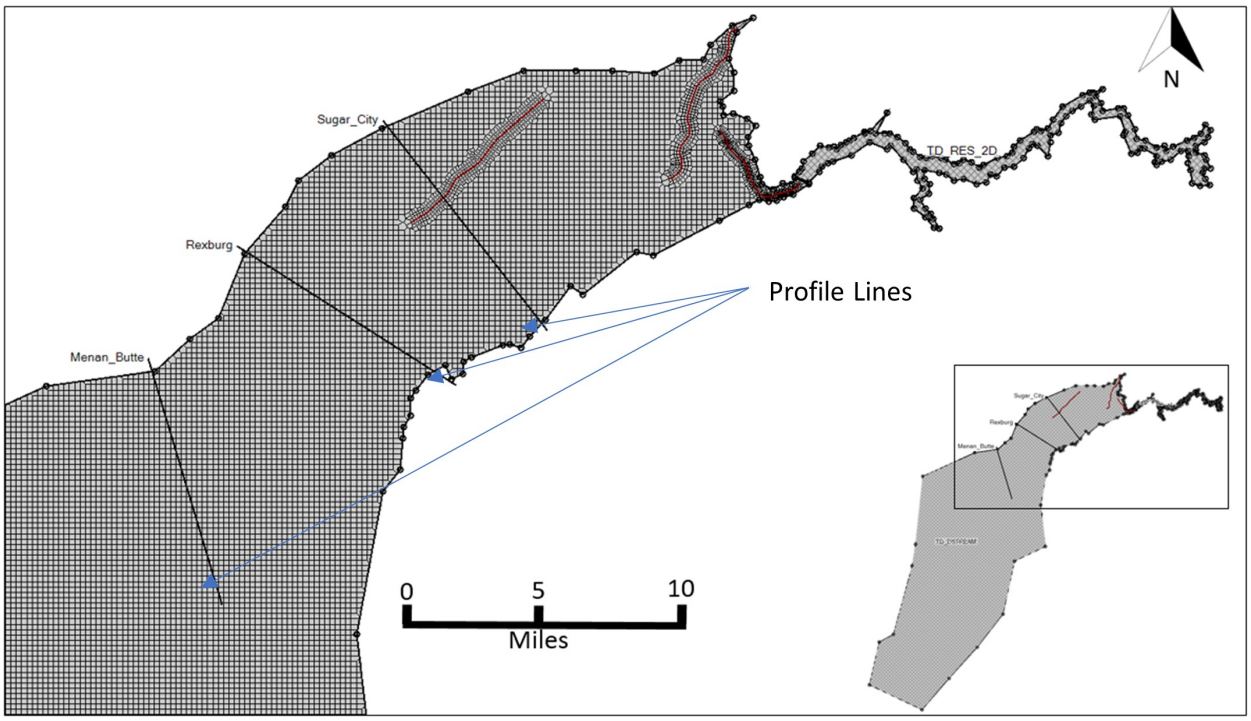

Figure A.15: Three breaklines were inserted into the HEC-RAS downstream mesh, denoted in this image of the domain.